



**IJOER**  
RESEARCH JOURNAL

ISSN  
2395-6992

# International Journal of Engineering Research & Science

[www.ijoer.com](http://www.ijoer.com)  
[www.adpublications.org](http://www.adpublications.org)

Volume-6! Issue-3! March, 2020

[www.ijoer.com](http://www.ijoer.com) ! [info@ijoer.com](mailto:info@ijoer.com)

## Preface

We would like to present, with great pleasure, the inaugural volume-6, Issue-3, March 2020, of a scholarly journal, *International Journal of Engineering Research & Science*. This journal is part of the AD Publications series *in the field of Engineering, Mathematics, Physics, Chemistry and science Research Development*, and is devoted to the gamut of Engineering and Science issues, from theoretical aspects to application-dependent studies and the validation of emerging technologies.

This journal was envisioned and founded to represent the growing needs of Engineering and Science as an emerging and increasingly vital field, now widely recognized as an integral part of scientific and technical investigations. Its mission is to become a voice of the Engineering and Science community, addressing researchers and practitioners in below areas

Chemical Engineering	
Biomolecular Engineering	Materials Engineering
Molecular Engineering	Process Engineering
Corrosion Engineering	
Civil Engineering	
Environmental Engineering	Geotechnical Engineering
Structural Engineering	Mining Engineering
Transport Engineering	Water resources Engineering
Electrical Engineering	
Power System Engineering	Optical Engineering
Mechanical Engineering	
Acoustical Engineering	Manufacturing Engineering
Optomechanical Engineering	Thermal Engineering
Power plant Engineering	Energy Engineering
Sports Engineering	Vehicle Engineering
Software Engineering	
Computer-aided Engineering	Cryptographic Engineering
Teletraffic Engineering	Web Engineering
System Engineering	
Mathematics	
Arithmetic	Algebra
Number theory	Field theory and polynomials
Analysis	Combinatorics
Geometry and topology	Topology
Probability and Statistics	Computational Science
Physical Science	Operational Research
Physics	
Nuclear and particle physics	Atomic, molecular, and optical physics
Condensed matter physics	Astrophysics
Applied Physics	Modern physics
Philosophy	Core theories

Chemistry	
Analytical chemistry	Biochemistry
Inorganic chemistry	Materials chemistry
Neurochemistry	Nuclear chemistry
Organic chemistry	Physical chemistry
Other Engineering Areas	
Aerospace Engineering	Agricultural Engineering
Applied Engineering	Biomedical Engineering
Biological Engineering	Building services Engineering
Energy Engineering	Railway Engineering
Industrial Engineering	Mechatronics Engineering
Management Engineering	Military Engineering
Petroleum Engineering	Nuclear Engineering
Textile Engineering	Nano Engineering
Algorithm and Computational Complexity	Artificial Intelligence
Electronics & Communication Engineering	Image Processing
Information Retrieval	Low Power VLSI Design
Neural Networks	Plastic Engineering

Each article in this issue provides an example of a concrete industrial application or a case study of the presented methodology to amplify the impact of the contribution. We are very thankful to everybody within that community who supported the idea of creating a new Research with IJOER. We are certain that this issue will be followed by many others, reporting new developments in the Engineering and Science field. This issue would not have been possible without the great support of the Reviewer, Editorial Board members and also with our Advisory Board Members, and we would like to express our sincere thanks to all of them. We would also like to express our gratitude to the editorial staff of AD Publications, who supported us at every stage of the project. It is our hope that this fine collection of articles will be a valuable resource for *IJOER* readers and will stimulate further research into the vibrant area of Engineering and Science Research.



Mukesh Arora  
(Chief Editor)

## **Board Members**

### **Mukesh Arora (Editor-in-Chief)**

BE(Electronics & Communication), M.Tech(Digital Communication), currently serving as Assistant Professor in the Department of ECE.

### **Prof. Dr. Fabricio Moraes de Almeida**

Professor of Doctoral and Master of Regional Development and Environment - Federal University of Rondonia.

### **Dr. Parveen Sharma**

Dr Parveen Sharma is working as an Assistant Professor in the School of Mechanical Engineering at Lovely Professional University, Phagwara, Punjab.

### **Prof.S.Balamurugan**

Department of Information Technology, Kalaignar Karunanidhi Institute of Technology, Coimbatore, Tamilnadu, India.

### **Dr. Omar Abed Elkareem Abu Arqub**

Department of Mathematics, Faculty of Science, Al Balqa Applied University, Salt Campus, Salt, Jordan, He received PhD and Msc. in Applied Mathematics, The University of Jordan, Jordan.

### **Dr. AKPOJARO Jackson**

Associate Professor/HOD, Department of Mathematical and Physical Sciences, Samuel Adegboyega University, Ogwa, Edo State.

### **Dr. Ajoy Chakraborty**

Ph.D.(IIT Kharagpur) working as Professor in the department of Electronics & Electrical Communication Engineering in IIT Kharagpur since 1977.

### **Dr. Ukar W.Soelistijo**

Ph D , Mineral and Energy Resource Economics, West Virginia State University, USA, 1984, Retired from the post of Senior Researcher, Mineral and Coal Technology R&D Center, Agency for Energy and Mineral Research, Ministry of Energy and Mineral Resources, Indonesia.

### **Dr. Samy Khalaf Allah Ibrahim**

PhD of Irrigation &Hydraulics Engineering, 01/2012 under the title of: "Groundwater Management Under Different Development Plans In Farafra Oasis, Western Desert, Egypt".

### **Dr. Ahmet ÇİFCİ**

Ph.D. in Electrical Engineering, Currently Serving as Head of Department, Burdur Mehmet Akif Ersoy University, Faculty of Engineering and Architecture, Department of Electrical Engineering (2015-...)

### **Dr. Mohamed Abdel Fatah Ashabrawy Moustafa**

Ph.D. in Computer Science - Faculty of Science - Suez Canal University University, 2010, Egypt.

Assistant Professor Computer Science, Prince Sattam bin AbdulAziz University ALkharj, KSA.

### **Dr. Heba Mahmoud Mohamed Afify**

Ph.D degree of philosophy in Biomedical Engineering, Cairo University, Egypt worked as Assistant Professor at MTI University.

### **Dr. Aurora Angela Pisano**

Ph.D. in Civil Engineering, Currently Serving as Associate Professor of Solid and Structural Mechanics (scientific discipline area nationally denoted as ICAR/08—"Scienza delle Costruzioni"), University Mediterranea of Reggio Calabria, Italy.

### **Dr. Faizullah Mahar**

Associate Professor in Department of Electrical Engineering, Balochistan University Engineering & Technology Khuzdar. He is PhD (Electronic Engineering) from IQRA University, Defense View, Karachi, Pakistan.

### **Dr. S. Kannadhasan**

Ph.D (Smart Antennas), M.E (Communication Systems), M.B.A (Human Resources).

### **Dr. Christo Ananth**

Ph.D. Co-operative Networks, M.E. Applied Electronics, B.E Electronics & Communication Engineering Working as Associate Professor, Lecturer and Faculty Advisor/ Department of Electronics & Communication Engineering in Francis Xavier Engineering College, Tirunelveli.

### **Dr. S.R.Boselin Prabhu**

Ph.D, Wireless Sensor Networks, M.E. Network Engineering, Excellent Professional Achievement Award Winner from Society of Professional Engineers Biography Included in Marquis Who's Who in the World (Academic Year 2015 and 2016). Currently Serving as Assistant Professor in the department of ECE in SVS College of Engineering, Coimbatore.

### **Dr. Maheshwar Shrestha**

Postdoctoral Research Fellow in DEPT. OF ELE ENGG & COMP SCI, SDSU, Brookings, SD  
Ph.D, M.Sc. in Electrical Engineering from SOUTH DAKOTA STATE UNIVERSITY, Brookings, SD.

### **Zairi Ismael Rizman**

Senior Lecturer, Faculty of Electrical Engineering, Universiti Teknologi MARA (UiTM) (Terengganu) Malaysia  
Master (Science) in Microelectronics (2005), Universiti Kebangsaan Malaysia (UKM), Malaysia. Bachelor (Hons.) and Diploma in Electrical Engineering (Communication) (2002), UiTM Shah Alam, Malaysia

### **Dr. D. Amaranatha Reddy**

Ph.D.(Postdoctoral Fellow,Pusan National University, South Korea), M.Sc., B.Sc. : Physics.

## **Dr. Dibya Prakash Rai**

Post Doctoral Fellow (PDF), M.Sc.,B.Sc., Working as Assistant Professor in Department of Physics in Pachhunga University College, Mizoram, India.

## **Dr. Pankaj Kumar Pal**

Ph.D R/S, ECE Deptt., IIT-Roorkee.

## **Dr. P. Thangam**

BE(Computer Hardware & Software), ME(CSE), PhD in Information & Communication Engineering, currently serving as Associate Professor in the Department of Computer Science and Engineering of Coimbatore Institute of Engineering and Technology.

## **Dr. Pradeep K. Sharma**

PhD., M.Phil, M.Sc, B.Sc, in Physics, MBA in System Management, Presently working as Provost and Associate Professor & Head of Department for Physics in University of Engineering & Management, Jaipur.

## **Dr. R. Devi Priya**

Ph.D (CSE),Anna University Chennai in 2013, M.E, B.E (CSE) from Kongu Engineering College, currently working in the Department of Computer Science and Engineering in Kongu Engineering College, Tamil Nadu, India.

## **Dr. Sandeep**

Post-doctoral fellow, Principal Investigator, Young Scientist Scheme Project (DST-SERB), Department of Physics, Mizoram University, Aizawl Mizoram, India- 796001.

## **Mr. Abilash**

MTech in VLSI, BTech in Electronics & Telecommunication engineering through A.M.I.E.T.E from Central Electronics Engineering Research Institute (C.E.E.R.I) Pilani, Industrial Electronics from ATI-EPI Hyderabad, IEEE course in Mechatronics, CSHAM from Birla Institute Of Professional Studies.





## **Mr. Varun Shukla**

M.Tech in ECE from RGPV (Awarded with silver Medal By President of India), Assistant Professor, Dept. of ECE, PSIT, Kanpur.

## **Mr. Shrikant Harle**

Presently working as a Assistant Professor in Civil Engineering field of Prof. Ram Meghe College of Engineering and Management, Amravati. He was Senior Design Engineer (Larsen & Toubro Limited, India).

## Table of Contents

S.No	Title	Page No.
1	<p><b>Economical Design for Dairy Farm Structures</b>  <b>Authors:</b> Ketan Subhash Goyal, Mr. Prabhat Kumar Gupta, Dr. M Helen Santhi</p> <p> DOI: <a href="https://dx.doi.org/10.5281/zenodo.3734000">https://dx.doi.org/10.5281/zenodo.3734000</a></p> <p> <b>DIN Digital Identification Number:</b> IJOER-MAR-2020-3</p>	01-09
2	<p><b>Calibration of Crop Coefficients and Evapotranspiration Rates in Semi-Arid and Sub-Humid Agro climates: Impact on Crop Water Requirement</b>  <b>Authors:</b> Kartik V Jakkannavar, Tejaswini N Bhagwat</p> <p> DOI: <a href="https://dx.doi.org/10.5281/zenodo.3734002">https://dx.doi.org/10.5281/zenodo.3734002</a></p> <p> <b>DIN Digital Identification Number:</b> IJOER-MAR-2020-4</p>	10-23
3	<p><b>Heat Transfer and Unsaturated Flow Phenomena in Rigid Dual-Scale Porous Media</b>  <b>Authors:</b> Nirmal Kumar Balaguru, M. Jeyameena</p> <p> DOI: <a href="https://dx.doi.org/10.5281/zenodo.3734006">https://dx.doi.org/10.5281/zenodo.3734006</a></p> <p> <b>DIN Digital Identification Number:</b> IJOER-MAR-2020-6</p>	24-35
4	<p><b>Study of the Nickel Complex Formation with Citric Acid in A Mixture Alkyl Polyglycoside10 (APG10) Surfactant/Water System</b>  <b>Authors:</b> Do Xuan Truong, Nguyen Van Hoang, To Van Thiep</p> <p> DOI: <a href="https://dx.doi.org/10.5281/zenodo.3734010">https://dx.doi.org/10.5281/zenodo.3734010</a></p> <p> <b>DIN Digital Identification Number:</b> IJOER-MAR-2020-10</p>	36-41

# Economical Design for Dairy Farm Structures

Ketan Subhash Goyal<sup>1</sup>, Mr. Prabhat Kumar Gupta<sup>2</sup>, Dr. M Helen Santhi<sup>3</sup>

P.G. student, Division of Structural Engineering,

School of Mechanical and Building Sciences, VIT University, Chennai Campus, Chennai, India

Principal Engineer and Owner, ACE consulting engineers, Pune

Professor, School of Mechanical and Building Sciences, VIT University, Chennai Campus, Chennai, India,

**Abstract**— In this study a steel framed dairy farm structure designed by considering IS 800-2007. It has been observed that by following the code recommendations for the design of dairy farm structures, it becomes expensive, that an ordinary farmer can't afford it. The basic idea of the investigation is to make these structures more economic for the farmers so that they become affordable. It is proposed to take realistic approach viz-a-viz applicable codes in design of these structures to make them safe and economical. The analysis and design will be done using ETABS software. The factors such as structural capacity and cost involved will be focused in the study.

**Keywords**— Dairy Farm, Economic Design, Realistic Loads, Quantity Comparison.

## I. INTRODUCTION

India is agrarian country. Agriculture is the profession of more than 75% of the population of the country and dairy farming comes along with it. Dairying is an important source of subsidiary income to small/marginal farmers and agricultural labors. Dairy producers aim to ensure that the safety and quality of their raw milk will satisfy the highest expectations of the food industry and consumers.

The total milk production in the country for the year 2018-19 was estimated at 189 million metric tonnes and the demand is expected to be 230 million tonnes by 2022. To achieve this demand annual growth rate in milk production has to be increased from the present 6.5 % to 9%. Thus, there is a tremendous scope for increasing the milk production through profitable dairy farming. Thus, understanding the requirements for dairy farm structures gain attention of this study.

This includes study of geometry of structure. The structure is used mainly by animals for living purpose. Different areas are to be made for resting and feeding them. These structures are situated in farms which are plain terrains. All these put challenges in selecting the shape and size columns. Therefore, careful designing is essential.

The productivity of animals in India is not as much to justify the cost of production of safe milk. Therefore, farmers look for lower costs. Even the financial institutions stress to lower the cost for better feasibility and sustainability of these farms. Hence the thorough study is needed to lower down the costs of these structures.

## II. LITERATURE REVIEW

Indian Standard Recommendations for Cattle Housing for Large Dairy farms <sup>[12]</sup> in 1970 suggested that better breeding coupled with selection, feeding and disease control, proper housing is an important feature in raising the productivity of animals. At present only a small proportion of cattle is maintained on scientific lines. Proper housing which is conducive to good health, comfort and protection from inclement weather, and which would enable the animals to utilize their genetic ability and feed for optimal production, is grossly lacking except at a few organized farms. India's climatic conditions, unlike most of the principal dairy countries of the world, are very varied. Hence designs of cattle sheds would also vary according to the climatic conditions prevailing in a particular region. To meet this requirement code has adopted the classification as plain areas with medium rainfall, heavy rainfall and high humidity areas, arid areas, and high altitude areas.

Indian Standard recommendations for Gaushala<sup>[15]</sup> in 1986 gave the general layout for dairy structures and various components of the structure. It gave the detail classification of each and every required area for dairy farm structure and defined all the terminologies used in dairy farming. It also provided site selection criteria.

S.K. Mosielele<sup>[20]</sup> in his "Dairy Farm Handbook" pictorially explained about different types of breeds of cows, the country in which the breed is developed, their nature, weights and per day milking capacities that helped in understanding the facts about different breeds so as to design the farm accordingly.



Indian standard recommendations for Cattle Housing in Rural areas<sup>[17]</sup> in 2005 provided recommendations for layout and constructional details of a cattle shed meant for an average farmer normally having three milch animals with their calves and a pair of bullock and rural milk producer normally having 20 animals which may include about 12 milch animals, their followers and a pair of bullocks.

International Dairy Federation in their research paper titled “Guide to Good Dairy Farming Practice”<sup>[4]</sup> in 2011 provided information about animal’s health, milking hygiene, animal’s nutrition that includes food and water, animal welfare, environment and socio-economic management. It is said that these practices must ensure that the milk and milk products produced are safe and suitable for their intended use, also that the dairy farm enterprise is viable into the future, from the economic, social and environmental perspectives. This study approaches to highlight relevant aspects that need to be proactively managed on dairy farms, to identify the desired outcomes in dealing with each of these areas, to specify good practice that addresses the critical hazards, and to provide examples of control measures that should be implemented to achieve the objectives. This Guide is intended as a resource for dairy farmers, to be used or implemented in a way that is relevant to their particular farming system. The focus is on the desired outcomes, rather than on specific, prescriptive actions or processes.

K. Suresh Kumar, C. Cini, Valerie Sifton<sup>[6]</sup> in their research paper “Assessment of design wind speeds for metro cities of India” recalculated the design wind speeds based on the local airport data. In this study it is seen that the design wind speeds for metro cities of India have been found to be about 5-10% lower than wind speed provided in Indian Standard. This can have significant impact on the prediction of wind induced loads of structures.

N. Lakshmanan, S. Gomathinayagam, P. Harikrishna, A. Abraham and S. Chitra Ganapathi<sup>[9]</sup> collected long-term data on hourly wind speed from 70 meteorological centres of Indian Meteorological Department. The daily gust wind data is processed for annual maximum wind speed for each site. Extreme wind value quantities have been derived using the Gumbel probability paper. A revised basic wind speed map for the country is suggested in which it is found that basic wind speed for most of the cities in India is found to much lower than the one suggested by Indian Standard.

American Society of Civil Engineers<sup>[1]</sup> in 2003 provided requirements for dead, live, soil, flood, wind, snow, rain, ice, and earthquake loads, and their combinations that are suitable for inclusion in building codes and other documents. Substantial changes were made to the wind, snow, earthquake, and ice provisions. In addition, substantial new material was added regarding the determination of flood loads. The structural loading requirements provided by this Standard are intended for use by architects, structural engineers, and those engaged in preparing and administering local building codes.

Indian Standard code of practice for design loads for building and structures IS: 875 (Part 2)-1987 for imposed loads.<sup>[16]</sup> By referring this code stepwise imposed loads are calculated for different components of dairy farm structure. This gave thorough and systematic method for finding out wind load intensities.

Roberto Mosheim and C. A. Knox Lovell<sup>[11]</sup> surveyed different farms based on the 2000 Agricultural Resource Management Survey, the most recent national survey of dairy producers in the United States. They employed a shadow cost function to decompose and analyze economic efficiency and scale economies. Preliminary results point to important scale economies and suggested that surviving small farms are on average more economically efficient but can exploit scale economies to a much lesser degree than larger farms.

Nikhil Agrawal, Achal Kr. Mittal, V. K. Gupta<sup>[10]</sup> in 2009 performed the load analysis by referring several different countries codes. For this analysis they have used Howe truss with different roof angles like 5°,10°,15°,20°, and 25° slopes. It has been observed that the minimum forces are obtained for 15° roof slope. Thus, in this study we are adopting 15° slope for roof slope.

Indian Standard Design Loads for Building and Structures – Code of Practice IS 875: (Part 3) -2015 for wind loads.<sup>[19]</sup> The wind load intensities for different components of the structure are calculated by the reference of this code.

Indian Standard General Construction in Steel- Code of Practice IS 800: 2007<sup>[18]</sup> gave the details regarding the steel design for various types of steel structures by both limit state and working stress method. It provided section properties for hot rolled sections.

James M. MacDonald, Erik J. O’Donoghue, William D. McBride, Richard F. Nehring, Carmen L. Sandretto, and Roberto Mosheim<sup>[5]</sup> in 2007 concluded in their paper Profits, Costs, and the Changing Structure of Dairy Farming that larger farms realize lower production costs. Although small dairy farms realize higher revenue per hundredweight of milk sold, the cost

advantages of larger size allow large farms to be profitable, on average, even while most small farms are unable to earn enough to replace their capital. On average, farms with at least 1,000 cows realize costs, per hundredweight of milk produced, that are 15 percent lower than farms in the next largest size class (500–999 head) and 35 percent lower than farms with 100–199 head. Other evidence suggests that costs may continue to decline as herds increase to and above 3,000 head.

Dejun LIU, Guangsheng ZHANG (2010),<sup>[2]</sup> used various sensors, automatic machines and intelligent technology (IT) applications make it possible to manage a dairy farm supply chain on a more detailed level than before and described a new system which can be used to develop an Intelligent Communication Technology (ICT) system as dairy farm management tools to describe, document and control all processes on dairy production. With the intelligent and integrated system, the farm managers never needed to operate several computers each day and manually transfer data from one unit to another, and even made more rational decision through acquiring amount of information.

Nicholas S Trahair (2012)<sup>[13]</sup> concluded that future designs might allow the use of purpose-built computer programme which can provide accurate predictions of members strength, and might only describe the characteristics of the methods of structural analysis and the member design strength which may be used. Such a code would have some of the present member strength inaccuracies and shortcomings removed and allow them to be replaced by the more accurate member strength computer programs.

Steffe Jerome and Grenter<sup>[14]</sup> in their paper namely Gilbert Information System for Farms using Precision Agriculture Techniques and EDI standards tried to define an up-dated general Information System for farming. This general Information System is based on a central module, to which are connected several peripheral thematic modules. One of these peripheral modules was designed for crop production, taking into account the needs of Precision Farming. Compatibility of this Information System with ISO standards for EDI in agriculture was tested, and a review of the critical points was carried out.

### III. DESIGN DETAILS

#### 3.1 Selection of type of Structure

As economy is major concern of this study, we have started with very basic structures like frame structures with different fixity at bases. Trials are conducted to arrive at final types of structure. Thus, after trying out different frames and trusses we arrived at Dual pitched roof truss with semi-rigid joints.

#### 3.2 Selection of suitable Roof Slope

While designing any industrial building with Pitched roof, studying roof slope is of paramount importance as it influences the components of loads acting on it. Thus, while moving for the design of dairy farm structures initially we focused on selection of roof slope. In IS 6027-1970 “Recommendation for Farm Cattle Housing for Large Dairy Farms” section A -5.1 it is suggested to adopt roof slope of 22 to 30°. But several studies says that roof slope of 15° is practically better.



FIGURE 1: Frame with 22° slope

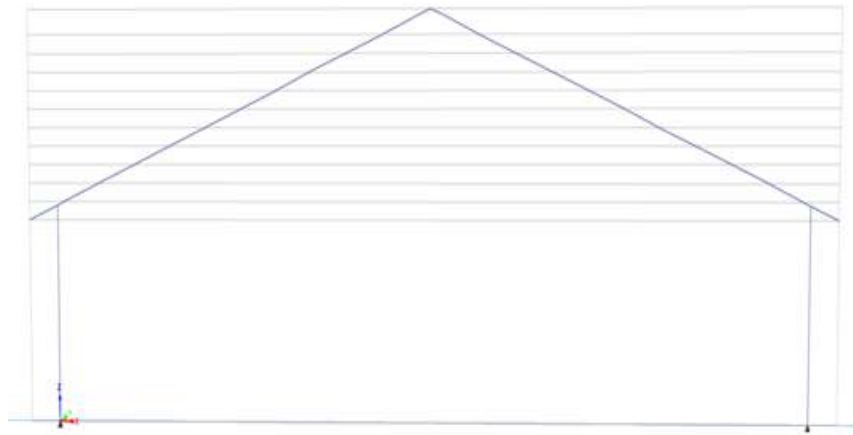


**FIGURE 2: Frame with 15° slope**

Thus, here we are going to take two different models with both 15° and 22° slopes.

### 3.3 Load Calculations

Load calculations are done separately for both designs. Thorough study of different loads and load combinations are done.

#### Loads calculation for 15° slope model

Economy can be achieved by considering loads which actually going to act on the structure and designing it for those specific loads. Thorough study is conducted for finding out realistic loads on the structure. Various Indian Standard codes and several research papers are referred. Load calculations were done as follows.

Dead Load,

$$\text{GI sheeting} = 0.037 \text{ kN/m}^2$$

$$\text{Fixings} = 0.025 \text{ kN/m}^2$$

Live Load, (As per IS: 875 Part 2 – 1987)

Adopted roof slope is 15° therefore from table no.2 of IS 875:1987 Part-2

For sloping roof with slope greater than 10°

$$0.75 - (0.2 \times 5) = 0.65 \text{ kN/m}^2 \text{ for purlins}$$

Wind Load, (As per IS: 875 Part 3 – 2015)

The Structure is considered to be located in Nashik city in Maharashtra.

Length = 58 m

Width = 26.66 m

Height = 7 m

$$V_z = V_b \cdot k_1 \cdot k_2 \cdot k_3 \cdot k_4$$

where  $V_b$  = Basic Wind Speed = 39 m/s

For Farm Structures,

Mean Probable design life = 25 years

$$k_1 = 0.92 \dots (\text{from Table 1})$$

$$k_2 = 1 \dots (\text{from Table 2}) \text{ for Cat 2}$$

$$k_3 = 1 \dots (\text{clause 6.3.3.1})$$

$$k_4 = 1 \dots (\text{clause 6.3.4})$$

$$V_z = 35.88 \text{ m/s}$$

$$P_z = 0.6 \times V_z^2 = 772.424 \text{ N/m}^2$$

Design wind pressure is,

$$P_d = K_d \cdot K_a \cdot K_c \cdot P_z \text{ or } 0.7P_z \text{ (whichever is higher)}$$

Where,  $K_d$  = wind Directionality factor = 0.9

$K_a$  = Area averaging factor = 1

$K_c$  = Combination factor = 1

$$P_d = 0.695 \text{ kN/m}^2$$

Net pressure co-efficient

(In X-direction)

Maximum positive roof pressure, (angel = 0) = +0.4

Maximum negative roof pressure. (angle = 0) = -0.8

Purlins spacing = 1.3 m

**TABLE 1**  
**NET PRESSURE CO-EFFICIENT IN X-DIRECTION.**

( $P_z \times \text{Area} \times \text{Co-eff.}$ )	Windward (kN)	Leeward (kN)
Intermediate	$0.695 \times 0.4 \times 1.3 = 0.361$	$0.695 \times (-0.8) \times 1.3 = -0.723$
End	$0.695 \times 0.4 \times 1.3/2 = 0.18$	$0.695 \times (0.8) \times 1.3/2 = -0.361$

Thus, horizontal and vertical components of windward and leeward forces on purlins for  $15^\circ$  slope can be found out as follows. Taking 10% less loads than calculated as per K. Suresh Kumar, C. Cini, Valerie Sifton paper.

**TABLE 2**  
**VERTICAL AND HORIZONTAL COMPONENTS OF NET PRESSURE CO-EFFICIENT (WL 1)**

	Components	Intermediate Purlins	End Purlins
Windward	Vertical ( $\cos 15^\circ$ )	-0.3141	-0.157
	horizontal ( $\sin 15^\circ$ )	0.0841	0.0421
Leeward	Vertical ( $\cos 15^\circ$ )	0.6285	0.3141
	horizontal ( $\sin 15^\circ$ )	0.168	0.084

(For Z-direction)

Roof pressure, (angel =  $90^\circ$ ) = -0.3

**TABLE 3**  
**COMPONENTS OF NET PRESSURE CO-EFFICIENT (WL 2)**

	Components	Intermediate Purlins	End Purlins
Windward	Vertical ( $\cos 15^\circ$ )	0.235	0.117
	horizontal ( $\sin 15^\circ$ )	-0.063	-0.0315
Leeward	Vertical ( $\cos 15^\circ$ )	0.235	0.117
	horizontal ( $\sin 15^\circ$ )	0.063	0.315

Seismic Load (IS -1893 part 4 -2005)

$$V_b = \text{Design Shear} = A_h \cdot W$$

$$A_h = (S_a/g) / (R/I)$$

To find  $S_a/g$

Natural period of vibration

$$T_a = 0.085 h^{0.75}$$

For steel frame

$$= 0.085 \times 8.976^{0.75}$$

$$= 0.4407 \text{ sec}$$

From Annex B IS 1893 Part 4 : 2005

$S_a/g = 2.5$  for Medium Soil

$I = 1$  (From Table 4 structural in Category 4)

$R = 5$  (For steel frame)

$A_h = 2.5/(5/1) = 0.5$

$V_b = 0.5 \times 16.44 = 8.22$  kN

Load calculations for 22° slope model.

Dead Load same as for 1<sup>st</sup> model

Live Load,

$0.75 - (0.2 \times 12) = 0.51$  kN/m<sup>2</sup> for purlins

Wind Load,

$P_d = 0.695$  kN/m<sup>2</sup>

Net pressure co-efficient (Calculated from Interpolation between 20° and 25° slopes)

(for X-direction)

Maximum positive roof pressure, (angel = 0) = +0.64

Maximum negative roof pressure. (angle = 0) = -0.94

Thus, horizontal and vertical components of windward and leeward forces on purlins for 22° slope can be found out as follows. considering full load as per codes.

**TABLE 4**  
**VERTICAL AND HORIZONTAL COMPONENTS OF NET PRESSURE CO-EFFICIENT (WL 1)**

	Components	Intermediate Purlins	End Purlins
Windward	Vertical (cos22)	-0.535	-0.277
	Horizontal (sin22)	0.217	0.108
Leeward	Vertical (cos22)	0.78	0.387
	Horizontal (sin22)	0.33	0.156

(for Z-direction)

roof pressure, (angel = 90) = -0.3

**TABLE 5**  
**COMPONENTS OF NET PRESSURE CO-EFFICIENT (WL 2)**

	Components	Intermediate Purlins	End Purlins
Windward	Vertical (cos22)	0.262	0.139
	Horizontal (sin22)	-0.07	-0.035
Leeward	Vertical (cos22)	0.262	0.139
	Horizontal (sin22)	0.07	0.035

Seismic Load same as for 15° slope.

Load Combinations

Following Load Combinations are considered for both the models.

1.2 x DL + 0.6 x LL + 1.2 x WL 1

1.2 x DL + 1.2 x LL

1.5 x DL + 1.5 x WL 1

1.5 x DL + 1.125 x LL

1.2 x DL + 1.2 x SL

1.2 x DL + 1.2 x LL + 1.2 x SL

1.5 x DL + 1.5 x WL 2

1.2 x DL + 0.6 x LL + 1.2 x WL 2

## IV. ANALYTICAL INVESTIGATION

### 4.1 Modelling

Two models one with  $15^\circ$  roof slope and  $22^\circ$  roof slope is made using E-tabs Software separately. Load calculations are done for individual models. 1<sup>st</sup> model is with  $15^\circ$  roof slope and wind loads for this model are considered as 10% lesser as suggested by K. Suresh et al., (2012). Loads are applied in both X and Z directions. Another model is with  $22^\circ$  roof slope is made as it is suggested to adopt  $22^\circ$  roof slope for dairy farm structure in an Indian Standard code. The wind loads applied on this model are as per Code.

### 4.2 Selection of sections

Sections are assigned on the basis of trial and error method. Both the models have enough strong sections to withstand loads. Design and analysis are done and total quantity of steel is found out. The final design for both the models and analysis is done using E-tabs Software. 3-D view of the  $15^\circ$  and  $22^\circ$  roof slope model is as pictured below.

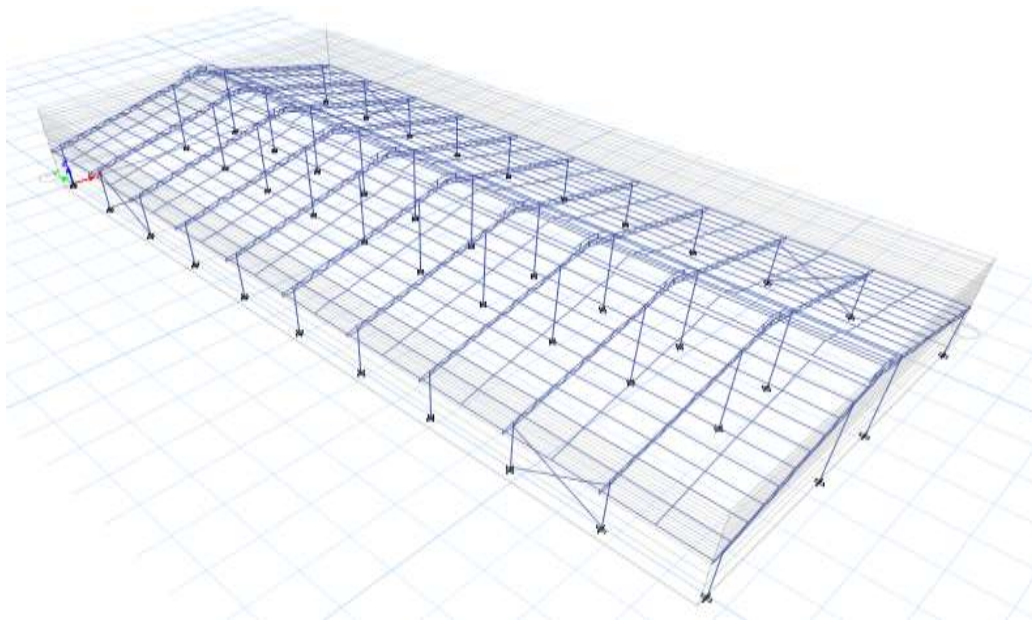


**FIGURE 3:  $15^\circ$  roof slope model**

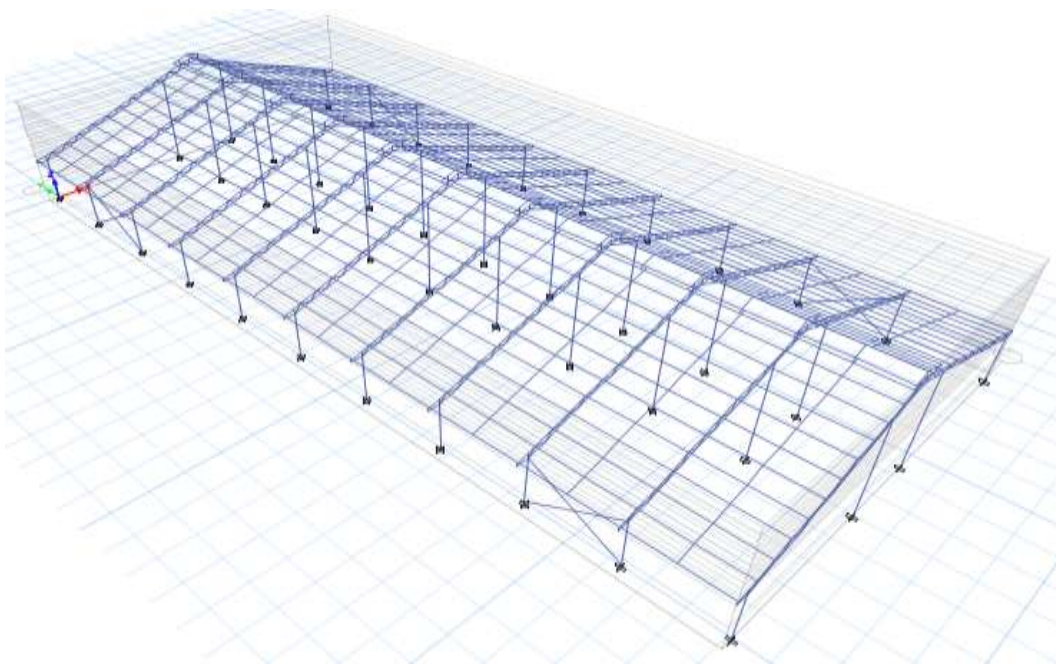


**FIGURE 4:  $22^\circ$  roof slope model**

## V. RESULTS AND DISCUSSION

From Literature study it can be understood that 15° roof slope model proves better in saving material than 22° roof slope model, which is suggested by dairy farming code also minimum forces are obtained with 15° slope, and hence adopted.

Several Studies revealed that the wind load study code in India has not been updated since years and the actual load are approximately 5-10% of that suggested in codes . The 15° slope model is designed using 10% lesser loads than that on another model. As loads decreases smaller truss sections can be used.

The steel consumed by both the models is as displayed in tables below.

**TABLE 6**  
**TYPES OF SECTIONS USED FOR BOTH THE MODELS ARE DISPLAYED IN TABLE BELOW.**

	Truss Member		Assigned Property	
	22° roof slope model	15° roof slope model	22° roof slope model	15° roof slope model
External Columns	ISMB300	ISMB250	ISMB300	ISMB250
Internal Columns	TUB1001004	TUB1001004	TUB1001004	TUB1001004
Columns For Skylight	TUB45452.6	TUB30302.6	TUB45452.6	TUB30302.6
Upper and Bottom chord members	PIP1397M	PIP603M	PIP1397M	PIP603M
Web Members	PIP483M	PIP337L	PIP483M	PIP337L
Purlins	ISMC150	ISMC125	ISMC150	ISMC125
Bracings	TUB63634.5	TUB63634.5	TUB63634.5	TUB63634.5
Sag Rods	Cir 0.01	Cir 0.01	Cir 0.01	Cir 0.01

**TABLE 7**  
**TABLE OF COMPARISON FOR QUANTITY OF STEEL**

Model	22° roof slope	15° roof slope
Quantity of steel	47.1 tonnes	29.66 tonnes

## VI. CONCLUSION

- It is observed that 15° roof slope proves ideal for designing of dairy farm shed.
- The reduced wind loads made it possible to reduce section sizes to very small as compared to conventional 22° roof slope model.
- The total savings in quantity of steel is found to be close to 30%.

## REFERENCES

- [1] American Society of Civil Engineers, "Minimum Design Loads for Buildings and Other Structures", American Society of Civil Engineers, 2003
- [2] Dejun LIU, Guangsheng ZHANG, "Study of Information Feasibility and Dairy Farm Information Management System", Logistics for Sustained Economic Development © 2010 ASCE.
- [3] Krishna, P., "Wind loads on low rise buildings - A review", Journal of Wind Engineering and Industrial Aerodynamics, Vol. 54-55, pp. 386-396, 1995.
- [4] Helen Dornom and Rejean Bouchard, "Guide to Good Dairy Farming Practice", Food And Agricultural Organisation of the United Nations and International Dairy Federation Rome, 2011.
- [5] James M. MacDonald, Erik J. O'Donoghue, William D. McBride, Richard F. Nehring, Carmen L. Sandretto, and Roberto Mosheim, "Profits, Costs, and the Changing Structure of Dairy Farming", Economic research report (United States. Dept. of Agriculture. Economic Research Service); no. 47, Sept 2007.
- [6] K. Suresh Kumar, C. Cini, Valerie Sifton, "Assessment of design wind speeds for metro cities of India", The Seventh International Colloquium on Bluff Body Aerodynamics and Applications Shanghai China, sept. 2012
- [7] L. Aurelius, and S. Cammelli, "A detailed assessment of Design wind speeds for Mumbai, 13<sup>th</sup> International conference of Wind Engineering, Amsterdam, 2011.
- [8] Mittal, Achal Kr., "Collapse of an industrial shed under wind loads possible causes and remedial measures- A case study", Fourth National Conference on Wind Engineering NCEW-2007
- [9] N. Lakshmanan, S. Gomathinayagam, P. Harikrishna, A. Abraham and S. Chitra Ganapathi, "Basic wind speed map of India with long-term hourly wind data Current Science, Vol. 96, No. 7, 2009.

- 
- [10] Nikhil Agrawal, Achal Kr. Mittal, V. K. Gupta, "Design of Gable Frame based on Wind Forces from a few International Design Wind Codes", The Seventh Asia-Pacific Conference on Wind Engineering, Taipei, Taiwan, Nov 8-12, 2009.
- [11] Roberto Mosheim and C. A. Knox Lovell, "Economic Efficiency, Structure and Scale Economies in the U.S. Dairy Sector", American Agricultural Economics Association Annual Meeting, Long Beach, California, July 23-26, 2006.
- [12] Nicholas S Trahair, "Trends in the Analysis and Design of Steel Framed Structures", Research report R926, The University of Sydney, Feb. 2012.
- [13] Steffe Jerome and Greuter Gilbert, "Information System for Farms using Precision Agriculture Techniques and EDI standards", Information System Laboratory ENITA de Bordeaux, France, 2010.
- [14] Indian Standard IS: 11942, "Indian Standard recommendations for Gaushala", Bureau of Indian Standards, New Delhi, July 1987.
- [15] Indian Standards IS: 875 Part 2, "Indian Standard code for practice for Design Loads (other than Earthquake) for Buildings and Structures Imposed Loads", Bureau of Indian Standards, New Delhi, Second Edition, June 1987
- [16] Indian Standards IS: 11799, "Indian Standard Recommendation for Cattle Housing in Rural Areas", Bureau of Indian Standards, New Delhi, First Edition, May 2005.
- [17] Indian Standards IS: 800, "Indian Standard general construction in steel- Code of Practice", Bureau of Indian Standards, New Delhi, Third Revision, Dec 2007.
- [18] IS: 875 Part 3, "Design Loads (other than Earthquake) for Buildings and Structures- Code for Practice Wind Loads", Bureau of Indian Standards, New Delhi, Third Revision, 2015.
- [19] Indian Standards IS: Criteria for Earthquake Resistant design of Structures, Part 1 General Provision for buildings Fifth Revision, June 2007.
- [20] S.K. Mosielele, "Dairy Farm Handbook".



# Calibration of Crop Coefficients and Evapotranspiration Rates in Semi-Arid and Sub-Humid Agro climates: Impact on Crop Water Requirement

Kartik V Jakkannavar<sup>1</sup>, Tejaswini N Bhagwat<sup>2\*</sup>

<sup>1</sup>PG Student, U B D T College of Engineering, Davanagere, Karnataka.

<sup>2</sup>Associate Professor, U B D T College of Engineering, Davanagere, Karnataka.

\*Corresponding Author: Tejaswini N Bhagwat

**Abstract:** Crop water requirement, a key component for Irrigation planning and management depends on Actual Evapotranspiration rates. Variations in Evapotranspiration rates depends on the climatic conditions for a given soil and crop. The objective of this work is to determine the water consumptive use based on crop coefficients for Tomato in Semi-arid and Sub-humid agro climates. The Actual Evapotranspiration was quantified by Lysimeters. Sieve analysis of the soil indicated as sandy soil and has density of  $1.859 \times 10^{-3} \text{ Kg/cm}^3$ . Depending on density and the root depth of tomato crop, lysimeter of dimensions 52cm depth and 36cm diameter is used to measure actual evapotranspiration rate.

Regression analysis carried out for the actual evapotranspiration rates, computed using empirical formula indicated that the FAO-56 PM method is well suited for both the regions having correlation coefficients of 0.94 and 0.92 for Semiarid and sub-humid regions respectively. Further, it was found that Thornthwaite equation being the next suited method has a correlation of 0.90 for semiarid and Hargreaves method the next suited method with correlation of about 0.90 for sub-humid. Crop coefficients used in all this potential Evapotranspiration methods were calibrated with lysimeter insitu measurements.

The crop coefficients vary depending on the different crop stages. The recalibrated crop coefficients for tomato crop are 0.78, 1.045, 1.95 and 1.54 for initial, development, mid and late respectively for Semi-arid Agro-climate. Similarly for Sub-Humid agro climate the crop coefficients were found to be 0.9, 0.98, 1.55 and 1.3 respectively.

**Keywords:** SemiArid and Sub Humid regions, Evapotranspiration rates, calibrated crop coefficients, Tomato crop.

## I. INTRODUCTION

Fresh water is a finite resource, is limited in summer and the demand for Agriculture is continuously increasing in Asian countries (Ravikumar et al., 2011). Water availability for agriculture depends on climate and the different losses in the existing water cycle. It is well known that water is a major issue almost in all parts of the world especially for countries that have high population growth rates and thus more crop yield (Dinar et al., 2019). Water deficit owing to the temporal-spatial inconsistency between water supply and demand is expected to become harsh in present scenario. Recently, climate changes has shown imbalance in the losses like evapotranspiration rates, thus varying delta for the crop growth (GoI 2016; Surendran, 2019). Development of irrigation systems with efficient use of water is essential for the sustainability of the crop production system and accurate estimation of crop water use (evapotranspiration) is also a critical component for water resource management (Petrooulos et al., 2018). Evapotranspiration rates, one of the key components required for rainfall runoff modeling, reservoir management and other integrated approaches in agriculture dominating watersheds (Danlu et al., 2016). A better understanding of trends in potential evapotranspiration ( $ET_0$ ) is crucial for scientific management of water resources in varied Agro climates (Dinpashoh et al., 2018).

Accurate estimations on crop water requirement are needed to avoid the excess or deficit water application, with consequent impacts on nutrient availability for plants, soil salinity and groundwater contamination. Evapotranspiration ( $ET$ ) is an important component in water-balance models and irrigation scheduling, and is often estimated in a two-step process. The evaporative demand of the environment is estimated based on weather conditions, and is often estimated as the evapotranspiration from a theoretical, reference grass crop ( $ET_0$ ) with the crop defined as an actively growing, uniform surface of grass, completely shading the ground, and not short of water. The  $ET_0$  value is then adjusted to estimate the evapotranspiration of the particular crop of interest using a crop-specific crop coefficient (Fisher and Pringle, 2013)

Evapotranspiration varies with time, distance and altitude, a number of studies have attempted to investigate the trend of evapotranspiration rates ((Dinpashoh et al., 2018). The various factors affecting the rate of evapotranspiration depend on Weather parameters, Crop factors and Management and environmental conditions. Upon Identification of the best alternative

methods for each climate, our intention was to develop regression equations, which could serve as practical tools for estimation of  $ET_C$  values estimated by the simpler methods (Nandageri, 2006).

Reference evapotranspiration and crop evapotranspiration are the two types of evapotranspiration which are been defined by the Food and Agriculture Organization (FAO 56). The evapotranspiration rate from a reference surface, not short of water, is called the reference crop evapotranspiration or reference evapotranspiration and is denoted as  $ET_0$ . The reference surface is a hypothetical grass reference crop with specific characteristics. The crop evapotranspiration under standard conditions, denoted as  $ET_c$ , is the evapotranspiration from disease-free, well fertilized crops, grown in large fields, under optimum soil water conditions, and achieving full production under the given climatic conditions (Allen et al., 1998).  $ET_0$  depends on various factors like Weather parameters, Crop factors, Management and environmental conditions.  $ET_0$  depends only on the climatic conditions and expressing the evaporation power of the atmosphere. While,  $ET_C$  depends on the environment and management factors under the given climatic conditions.

There exist a multitude of methods for the estimation of potential evapotranspiration  $ET$  and free water evaporation  $E$ , which can be grouped into five categories: (1) water budget, (2) mass-transfer, (3) combination, (4) radiation (e.g. Priestley and Taylor, 1972), and (5) temperature-based (e.g. Thornthwaite, 1948; Blaney-Criddle, 1950). The availability of many equations for determining evaporation, the wide range of data types needed, and the wide range of expertise needed to use the various equations correctly make it difficult to select the most appropriate evaporation method for a given study (Xu and Singh, 2002). Hence there is a need to assess evapotranspiration losses for given soil conditions that has implications on efficient water resource management in basins experiencing varied agro climates.

Crop coefficient does not only vary with climate but in combination with crop stage. Irrigation frequency and water supply for each watering depends on crop stage besides evapotranspiration rates, thus crop coefficients are to be computed in combination with climate parameters as well as crop stage (Seidel et al., 2019).

## II. MATERIALS AND METHODOLOGY

First stage of the study comprises of the most commonly used empirical methods for estimating Evapotranspiration. Empirical based values were evaluated and compared within each category and the best and good methods are ranked for two dominant agroclimates of Karnataka (Figure. 3). In the second stage of the research, comparison is made for the evapotranspiration rates that are mass-transfer based, radiation-based and temperature based, respectively. Weather parameters for representative selected study site for Semi-arid and Sub-humid regions were collected from the website of Karnataka State Natural Disaster Monitoring Center and using the empirical formula, potential evapotranspiration rates for tomato crop is computed. Soil core samples collected from the spatially dominant soil group in the Semi-Arid agro climate were analyzed in the laboratory for its physico-chemical parameters and therefore the same soil conditions were maintained in both the agro climates. Lysimeter was setup in both the Agro climates to compute the Actual  $ET$  rates having similar root zone depth (40 cm). Regression analysis is attempted to understand the best fit model for each agro climate (Figure.1).

### 2.1 Experimental Setup

#### 2.1.1 Lysimeter Pot

A small Drum with 52cm depth and 36 cm diameter (Figure 2) is used as micro lysimeter, the depth of the lysimeter is decided upon the maximum rooting depth of the crop, Hence providing a sufficient depth for attaining the root growth.

#### 2.1.2 Water Storage Container

A 10 l polyethylene container is used to collect drained water. The excess water after satisfying the water holding capacity of soil and plant needs, gets percolated at the bottom and then accumulates in this container. For ease of recording the amount of water accumulated, Graduations in ml is marked on it. This container is placed in a trench below the foot level of lysimeter drum and also preventing evapotration of collected water.

After the installation, the drum is filled with a measured quantity of soil. The quantity of soil is measured on the basis of density of soil. It is such that the field density is maintained into the lysimeter which is of about  $1.859 \times 10^{-3} \text{ kg/cm}^3$  and 98.48 kg of soil is filled in the lysimeter. A measured quantity of water is irrigated on a daily basis or in an interval of time and the tomato seeds are allowed to germinate. In this study, the irrigation is provided about 3lts of water for every 2 days. the water loss due to evapotranspiration can be determined by simple calculation i.e. the difference of total water added by irrigation, rainfall or both and the excess water collected into the collecting tank at the bottom through percolation.

$$ET_c = WA + R - WP$$

Where,  $ET_c$ : Crop evapotranspiration,  $WA$ : Water added,  $R$ : Rainfall,  $WP$ : Water percolated

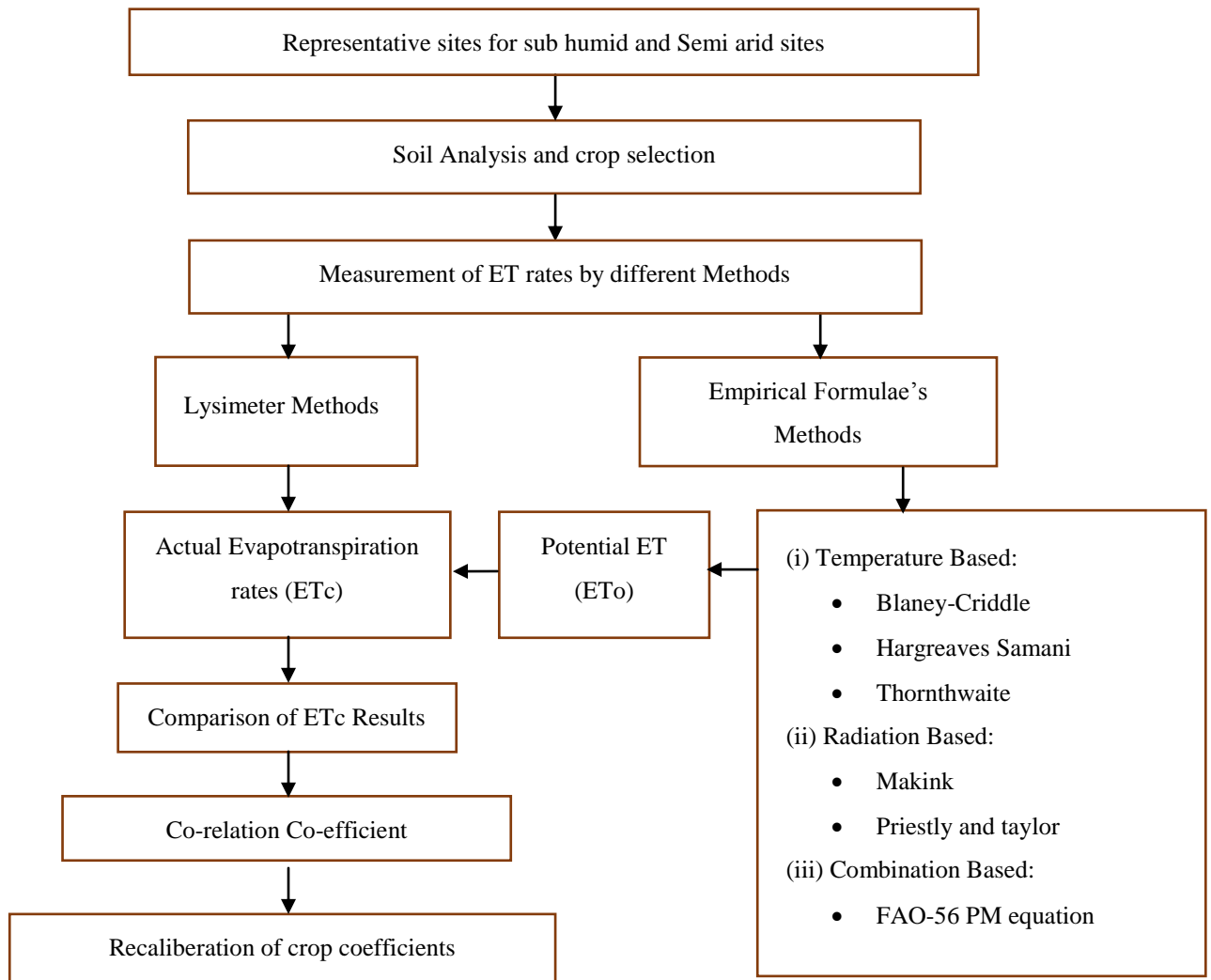


**FIGURE 1: Methodology flow chart of the study**



(a)



(b)

**FIGURE 2: Lysimeter Setup in both regions (a) Semi-Arid region, (b) Sub-Humid region.**

### III. PILOT STUDY

This study was carried out in two agro climatic regions during the period from March - June (2019) and the lysimeter were setup in both the regions. The first station “Devarabelekere” is an experimental farm representative site for Semi-Arid tropical climate. The farm is located at the city limits between Davanagere and Malebennur (Karnataka, India) and its average geographical coordinates are latitude  $14.47^{\circ}$  N, longitude  $75.91^{\circ}$ E and the altitude is 602.5 m above sea level (Figure.3). The Semi-arid region having average temperatures in the coldest month (July) of  $5.7^{\circ}\text{C}$  and in the hottest month (March) of  $46.9^{\circ}\text{C}$  approximately. During this study period the mean daily temperature was  $29.5^{\circ}\text{C}$ ; the degree of sunshine was high with an average of 12.4 hr/day.

“Balekundri” represents Sub-Humid region which is located between the Belgaum city and Marihal village. Its coordinates lie between Latitude:  $15.88^{\circ}$  N, Longitude:  $74.52^{\circ}$  E and at an elevation 751 m above sea level (Figure 3). The surroundings are fully representative of irrigated land in the area. Data are available on thermal and water characteristics of the area over a long period of time. Moreover, the data correspond to the period in which the experiment took place, were obtained from automated agro climatic stations. In the same way, Sub-Humid region has average temperatures in the coldest month (January) of  $4^{\circ}\text{C}$  and in the hottest month (April) of  $39.5^{\circ}\text{C}$  approximately and during this study period the mean daily temperature was  $28.21^{\circ}\text{C}$ ; the degree of sunshine was high with an average of 12.51 hr /day.

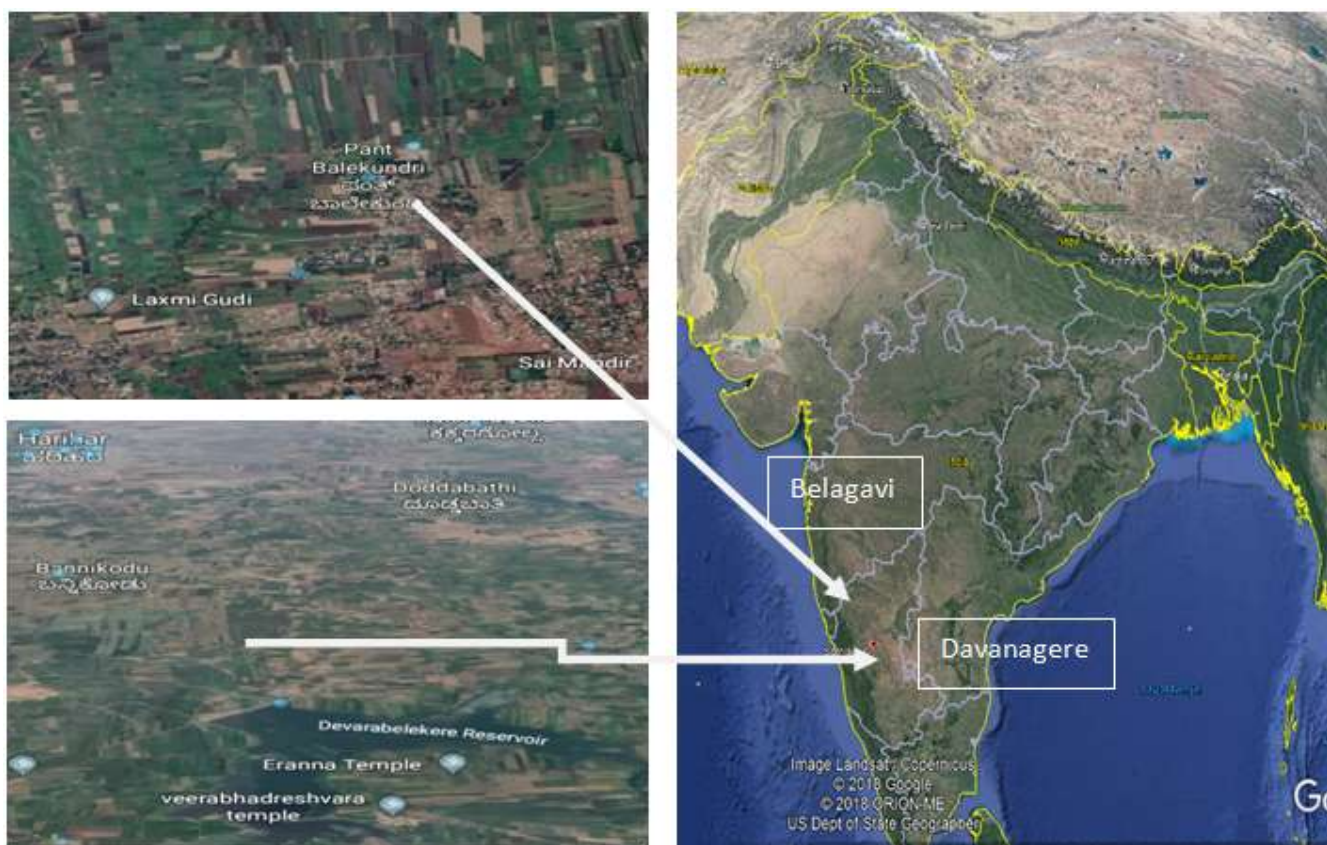


**FIGURE 3: Location of both the study area (i.e. Belagavi: Sub-Humid and Davanagere: Semi-Arid region) in Karnataka, India**

#### 3.1 Estimation by Empirical formula

When complete set of weather data required for the FAO-56 PM method are not available, procedures are described for using a reduced set of weather data as input. While air temperature measurements are almost always available, reliable measurements of solar radiation, relative humidity, and wind speed may not be. Extensive discussion and methods for estimating missing values are presented based on temperature measurements, historical and general knowledge of local environmental conditions. The reduced set of values, consisting of measured data and estimated values, is then input to the FAO-56 equation. In this study, this method was used to estimate ETo assuming the availability of maximum and minimum air temperatures only.

### 3.2 Weather parameters:

The weather parameters on which the Empirical formulae's rely are the daily recorded data's of Temperature, Humidity and Wind Speed, the same having average values are shown in the below (Table. 1).

**TABLE 1**  
**WEATHER PARAMETERS FOR SUMMER SEASON OF 2019.**

Month	Avg. Daily Temperature (°C)		Avg. Daily Humidity (%)		Avg. Daily Wind Speed (m/s)	
	S-A	S-H	S-A	S-H	S-A	S-H
March	29.6	28.03	41.97	57	1.65	1.77
April	30.61	29.08	50.06	58.6	2.48	1.98
May	29.91	29.12	58.80	59.41	3.52	3.07
June	27.87	26.60	67.75	73.87	4.39	3.86

*Note: S-A: Semi-Arid, S-H: Sub-Humid.*

The Average daily temperature and wind speed of Semi-arid region if found to have 1.29 °C and 0.34 m/s more than that of Sub-Humid region respectively. But the Humidity level is found to be 7.58% more in Sub-Humid region than semi-arid region. Hence the ET rates will tend to vary depending on these parameters in the respective agro climates.

Different reference evapotranspiration methods exist and range from direct measurement from a reference crop such as a perennial grass (Doorenbos and Pruitt, 1977) or computed from weather data using:

- Temperature models (Thornthwaite, 1948; Doorenbos and Pruitt, 1977),
- Radiation models (Doorenbos and Pruitt, 1977; Hargreaves and Samani, 1985), and
- Combination models (FAO-56 PM) (Allen et al., 1998).

The standardized Penman–Monteith equation had been adopted and recommended for reference evapotranspiration estimation. The various methods adopted in this study are listed below: Crop water use is generally estimated by multiplying the reference evapotranspiration by pre-determined crop-specific coefficient, which is dependent on many factors, including irrigation regimes and management (Djaman and Irmak, 2013).

### 3.3 Temperature Based Models:

#### 3.3.1 BlaneyCriddle Method:

This method is suggested for areas where available climatic data cover air temperature data only. It requires only mean daily temperatures T (°C) over each month (Blaney and Criddle, 1962):

$$ET_o = p * (0.46T + 8) \text{mm/day} \quad (1)$$

Where, ET<sub>o</sub>: Reference evapotranspiration (mm/day), p: mean daily percentage (for the month) of total annual daytime hours for Northern Hemisphere, T: Mean daily temperature in (°C) over the month considered.

#### 3.3.2 Thornthwaite Equation:

Thornthwaite correlated mean monthly temperature with evapotranspiration as determined from water balance from valleys with sufficient moisture available for maintaining transpiration. To calculate Potential Evapotranspiration (PET) using Thornthwaite method, first the Monthly Thornthwaite Heat Index (i) calculation is required, using the following formula (Thornthwaite, 1948):

$$i = \left(\frac{t}{5}\right)^{1.514} \quad (2)$$

Where, t: mean monthly temperature

The Annual Heat Index (I) is calculated, as the sum of the Monthly Heat Indices (i):

$$I = \sum_{i=1}^{12} i \quad (3)$$

Potential Evapotranspiration (PET) estimation is obtained for each month, considering a month is 30 days long and there are 12 theoretical sunshine hours per day, applying the following equation:

$$PET_{noncorrected} = 16 * \left(\frac{10*t}{I}\right)^\alpha \quad (4)$$

$$\text{Where } \alpha = (675 * 10^{-9} * I^3) - (771 * 10^{-7} * I^2) + (1792 * 10^{-5} * I) + 0.49239 \quad (5)$$

Obtained values are later corrected according to the real length of the month and the theoretical sunshine hours for the latitude of interest, with the formula:

$$PET = PET_{noncorrected} * \frac{N}{12} * \frac{d}{30} \quad (6)$$

Where, N: Theoretical sunshine hours for each month and d number of days for each month

### 3.3.3 Hargreaves & Samani Equation:

The Hargreaves & Samani equation estimates ETo based on maximum and minimum air temperature, and is written as (Hargreaves and Samani, 1985):

$$ET_o = 0.023(0.408)(T_{\text{mean}} - 17.8)(T_{\text{max}} - T_{\text{min}})^{0.5} Ra \quad (7)$$

Where, Tmax = maximum air temperature (°C), Tmin = minimum air temperature (°C), Ra = extraterrestrial radiation (MJ·m<sup>-2</sup>), and 0.408 is a factor to convert MJ m<sup>-2</sup> to mm. Extraterrestrial radiation, Ra, is estimated based on the location's latitude and the calendar day of the year.

## 3.4 Radiation Based Models

### 3.4.1 Priestley-Taylor Equation

The PriestleyTaylor equation is a simplification of the original Penman method, where the aerodynamic term is replaced by an empirical coefficient, known as the Priestley-Taylor parameter (Priestley and Taylor, 1972). The method is expressed by:

$$ET_o = 1.26 * \frac{\Delta}{\Delta + \gamma} \left[ \frac{R_n - G}{\lambda} \right] \quad (8)$$

Where,  $\lambda$ : Latent Heat of Vaporization (2.45 MJ kg<sup>-1</sup>). In fact, the Priestley Taylor parameter varies with different vegetation types, soil moisture conditions, and strength of advection (Priestley and Taylor, 1972; Stannard, 1993), and should be calibrated for different environmental conditions.

### 3.4.2 Makkink Equation

Makkink equation was proposed in 1957 for estimating ET from grass, the equation stands as (Djaman et al., 2015):

$$ET = 0.61 * \frac{\Delta}{\Delta + \gamma} * \frac{R_s}{\lambda} - 0.12 \quad (9)$$

Where, Rs: Total Solar Radiation,  $\Delta$ : slope of Saturation Vapor Pressure curve,  $\gamma$ : psychrometric constant,  $\lambda$ : latent heat.

## IV. RESULTS AND DISCUSSIONS

### 4.1 Potential Evapotranspiration rates:

Reference evapotranspiration rates in both the regions by all the six methods are presented in table 2. It is observed that the ETo rates are less in sub humid region when compared to semi-arid region. The average ETo rates by FAO-56 PM equation are 7.18 and 6.98 mm/day in Semi-Arid and Sub-Humid region respectively where as Thornthwaite equation it is 5.43 and 4.9 mm/day in the respective regions. BlaneyCriddle method in 6.23 and 5.66 mm/day respectively, by Hargreaves Samanieqn: 5.62 and 5.81 mm/day respectively, by Priestly Taylor eqn: 7.13 and 6.9 mm/day respectively and lastly by Makkinkeqn it is found to be 5.33 and 5.31 mm/day respectively.

**TABLE 2**  
**POTENTIAL EVAPOTRANSPIRATION RATES BY EMPIRICAL EQUATIONS IN SEMI-ARID AND SUB-HUMID REGION.**

Month	FAO-56 PM		TW		BC		H&S		P&T		MK	
	S-A	S-H	S-A	S-H	S-A	S-H	S-A	S-H	S-A	S-H	S-A	S-H
Mar	7.03	6.72	5.71	4.86	6.08	5.64	5.71	6	6.69	6.56	5.33	5.24
Apr	8.01	7.19	5.54	5.11	6.22	5.77	6.74	6.27	6.86	6.98	5.5	5.42
May	8.15	7.61	5.36	5.12	6.35	5.77	5.63	6.39	7.36	7.04	5.41	5.4
June	5.54	6.43	5.12	4.52	6.27	5.46	4.41	4.58	7.61	7.03	5.08	5.18
Avg.	7.18	6.98	5.43	4.9	6.23	5.66	5.62	5.81	7.13	6.9	5.33	5.31

*Note: S-A- Semi-Arid region, S-H:- Sub Humid region, FAO-56 PM: Penman Monteith's method, TW: Thornthwaite method, BC: Blaney Criddle method, H&S: Hargreaves Samani method, P&T: Priestly and Taylor method, MK: Makkink method.*

## 4.2 Crop Factor:

In the case of ETo grass is used as the reference crop. However other crops may not use the same amount of water as grass, due to changes in rooting depth, crop growth stages and plant physiology. The crop coefficient (Kc) takes into account the crop type and crop development to adjust the ETo for that specific crop. There may be several crop coefficients used for a single crop throughout an irrigation season depending on the crop's stage of development.

Crop coefficient (Kc) for tomato for every growing stages of the tomato crop differs hence the Kc value used in this study are 0.45(initial stages), 0.75(development stage), 1.15(mid-stage) and 0.80(late stage) (Rowell and Soe, 2016).

## 4.3 Computation of ETc:

The actual Evapotranspiration rates for tomato crop by various empirical reference ET methods are calculated. These results are obtained by multiplying the reference evapotranspiration rates with the suitable crop coefficients. Hence, The Actual ET is estimated by using the crop coefficients of tomato mentioned above.

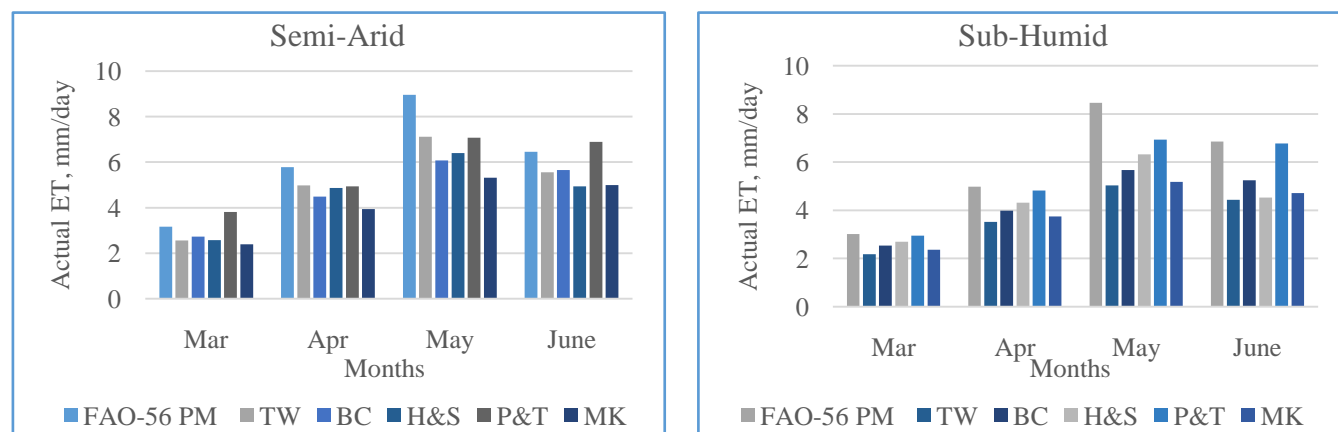


**FIGURE 4: Actual ET rates by Empirical formulae using crop coefficients**

The Actual Evapotranspiration rates is primarily dependent on the climatological factors. Hence we can see in figure 4 the variations in ETc rates due to greater temperature of about 1.29°C more in Semi-Arid region than that of Sub-Humid region, 7.57% lesser humidity in Semi-Arid than Sub-Humid and 0.39m/s greater wind speed in Semi-Arid region than Sub-Humid region. In Semi-Arid region, there is a slight increase in temperature of about 1.01°C in the month of April and the corresponding Humidity also increased of about 8.09% and also the wind speed of about 0.821 m/s. We can see that the ETc rates by various formulae, as the temperature increases the Priestly Taylor Equation falls down gradually and again when there is increase in temperature the same equation shows rising values. The Actual evapotranspiration rates by lysimeter method was found to be maximum at the development stage i.e. during the month of May of about 12.7 mm/day in semi-arid region and 10.7 mm/day in sub-Humid region. Average ETc is measured to be 8.40 and 7.77 mm/day in both regions respectively.

## 4.4 Insitu Methods: Lysimeter

Insitu evapotranspiration is measured using lysimeter. Lysimeter is defined as a device for measuring the percolation of water through soils and for determining the soluble constituents removed in the drainage. The water use (evaporation, transpiration, or ET) can be determined by a balance of the water above this boundary. Weighing lysimeters determine ET directly by the mass balance of the water as contrasted to non-weighing lysimeters which indirectly determine ET by volume balance.

## 4.5 Soil Analysis:

Lysimeters in both the agro climates are filled with the same type of soil (sandy soil) was used that has density of  $1.859 \times 10^{-3}$  kg/cm<sup>3</sup>. The water holding capacity is measured to be 40.02 lts (25gms = 10ml) and the moisture content of the soil was 1.61(Table 3). The pH and electrical conductivity of soil was measured to be 7.96 and 0.35 respectively. The nutrients concentration also was analyzed for Nitrogen, Phosphorous and Potassium, The obtained K value(21.94) (Table 3) is less than the 200 kg/ha which shows the soil has less K and not sufficient nutrient to grow plant. N(10.4), the limitations of N is 150-600 kg/ha, the N content of soil is below limitation is due to less N fixation and less microbial decomposition in soil. So

that the collected soil sample is not suitable for crop production. P(0.310) less than 5 kg/ha which shows the less content of P for growth of plant (Table 3).. Hence additional nutrients is applied during the growing stage of plants. The pH and Electrical conductivity was determined by the standard pH meter method and electrometric method which was found to have low electrical conductivity and slightly towards alkaline. The soil held water of about 10ml per 25 gms of soil and the nutrients level was also found to be present is less amount.

**TABLE 3**  
**SOIL PROPERTIES OF THE SAMPLE COLLECTED IN FIELD LOCATED IN SEMI-ARID**

Sl. No.	Characteristics	Values
1.	Soil type	Sandy soil
2.	Hp	7.96
3.	Electrical conductivity (dS/m)	0.35
4.	Density (kg/cm <sup>3</sup> )	1.859*10 <sup>-3</sup>
5.	Quantity of soil used (kg)	98.59
6.	Water Holding Capacity for 98.59kg (L)	40.02
7.	Moisture content	1.61
8.	Nitrogen (kg/Ha)	10.4
9.	Phosphorous (kg/Ha)	0.310
10.	Potassium (kg/Ha)	21.94

#### 4.6 Actual evapotranspirations Rates

In this Study an Experimental measurement of Evapotranspiration rates in the two regions mentioned above was performed using a typical tomato (*Lycopersicon esculentum*) crop, this crop having a base period of 90 to 150 days and is grown throughout the year and every season, Hence this crop was considered in this project. Simple Lysimeters were setup in both the regions. Materials used in this project are Soil, Plastic drum, Plastic Container, water pipe and Tomato seeds. Lysimeter observations for both Semi-arid and Sub-humid region are presented in Table 4.

**TABLE 4**  
**LYSIMETER OBSERVATIONS IN SEMI-ARID AND SUB-HUMID REGION**

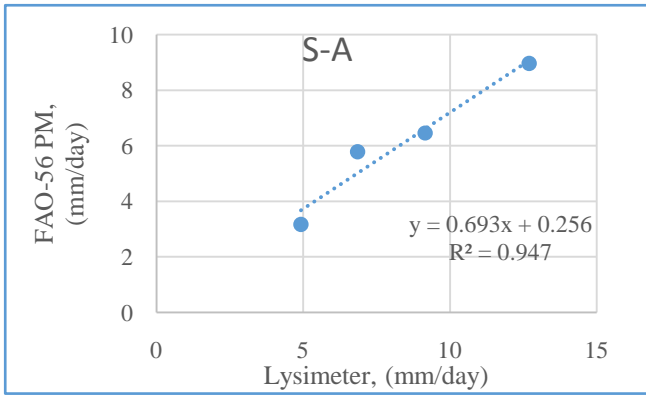
Month	Semi-Arid				Sub-Humid			
	Water Added (lt)	Rain fall (lt)	Water Drained (lt)	ETc (mm/day)	Water Added (lt)	Rain Fall (lt)	Water Drained (lt)	ETc (mm/day)
Mar	19	0.012	9.506	4.92	16	2.224	9.112	5.74
Apr	36	1.315	16.4	6.85	30	1.396	9.100	6.55
May	52	1.480	13.6	12.65	40	0.294	2.700	10.7
June	56	7.055	40.700	9.15	38	15.049	30.900	8.10
Total	163	9.862	80.206	8.39	124	18.963	51.812	7.77

The above lysimeter observations were recorded in both regions and the Average actual evapotranspiration rate of Tomato crop in Semi-Arid region is 8.39 mm/day and in Sub-Humid region it is 7.77 mm/day. This indicates more water requirement for crop growth in semi- arid region. Further, owing to rainfall in the month of June water required for the crop in sub humid region is less.

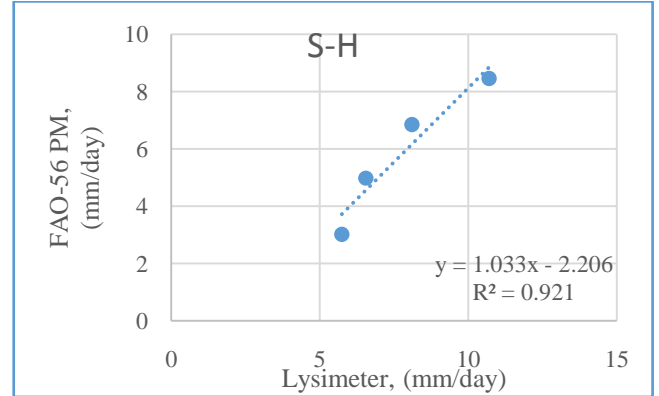
#### 4.7 Regression Analysis

The correlation amongst the Lysimeter method taken as independent variable and the various empirical methods taken as dependent variable, mathematically defines whether the average values of actual Evapotranspiration by lysimeter are interrelated to higher or lesser than average values of empirical methods.

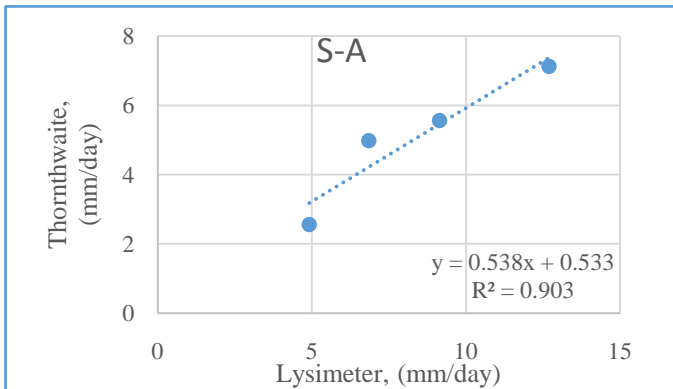




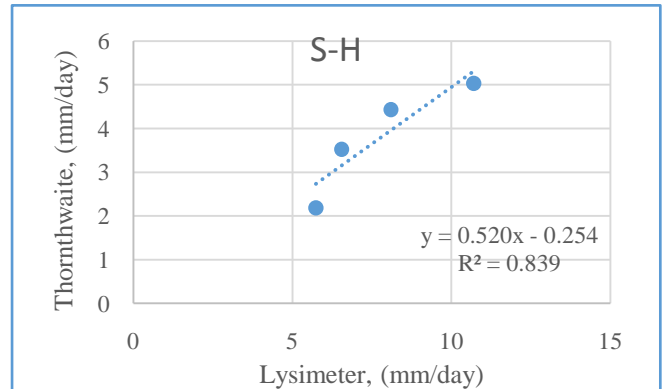
(a)



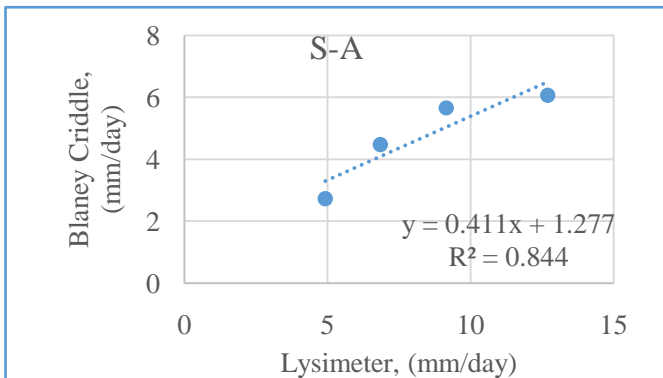
(b)



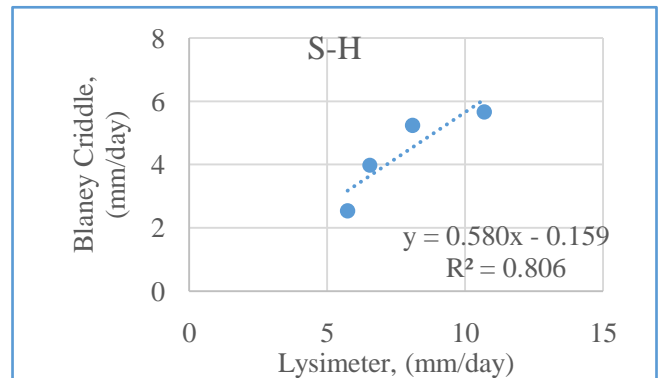
(c)



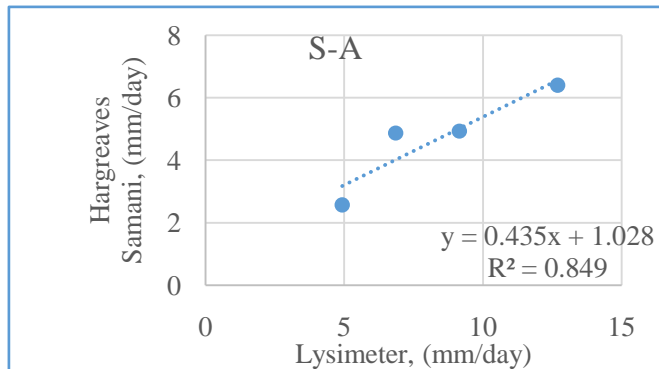
(d)



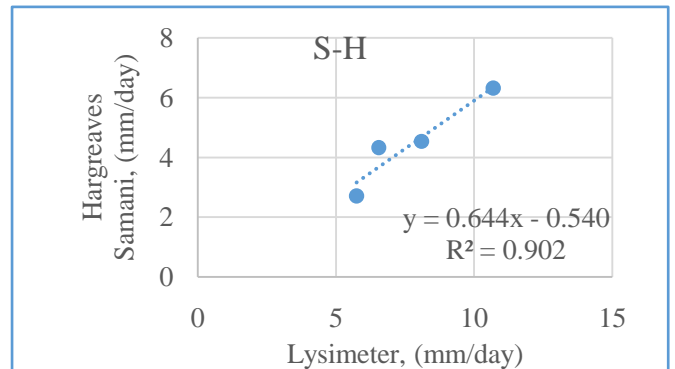
(e)



(f)



(g)



(h)

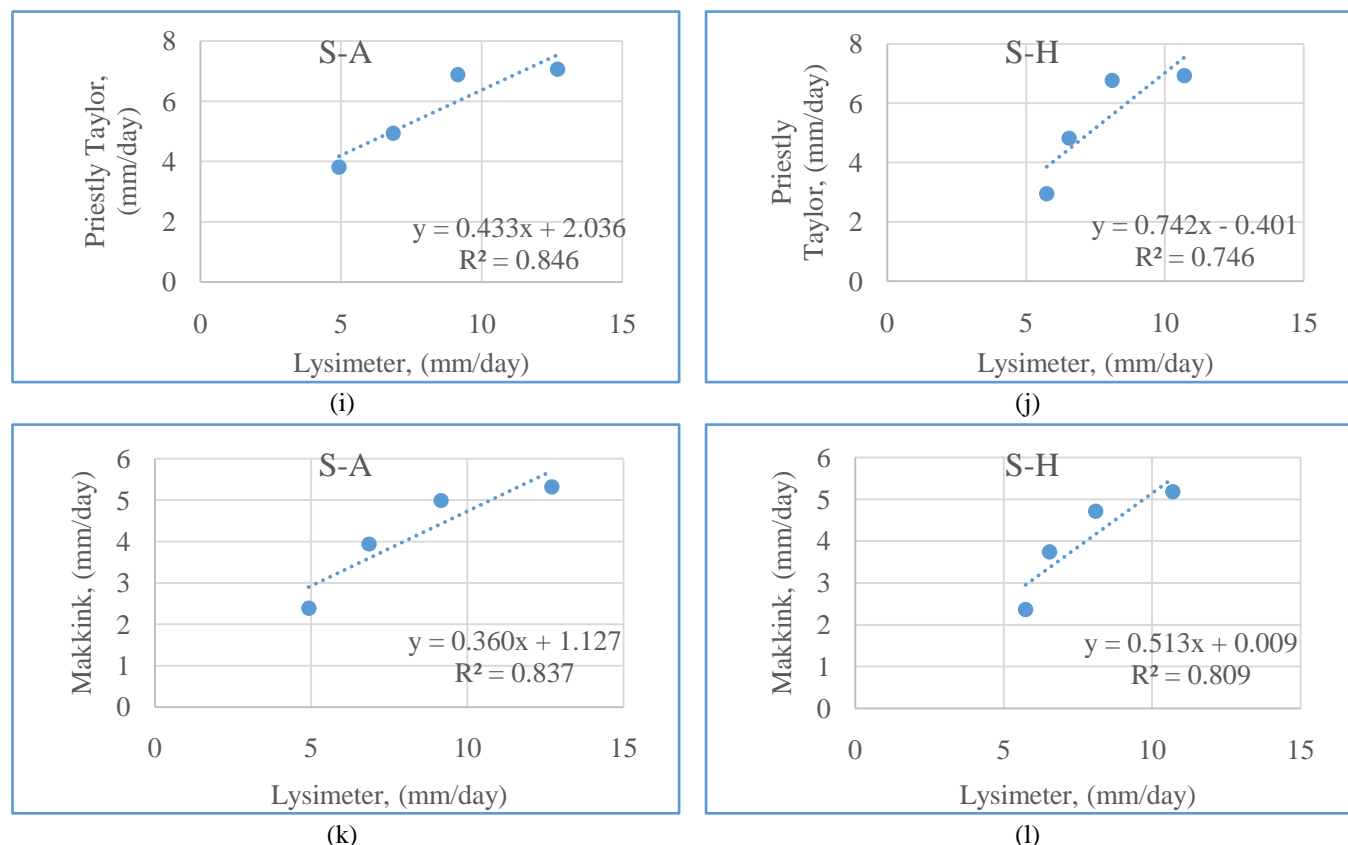


**FIGURE 5: Regression plots for various methods with respect to lysimeter method**

(Note:- S-A: Semi-Arid, S-H: Sub-Humid, fig 5(a & b): FAO-56 Penman Monteith method, Fig 5(c & d): Thornthwaite method, Fig (e & f): Blaney Criddle method, Fig5 (g & h): Hargreaves and Samani Method, Fig 5(i & j): Priestly and Taylor method, Fig5 (k & l); Makkink method).

Regression analysis indicates a good correlation for all the empirical methods (table 5). Amongst the empirical methods, The FAO-56 Penman Monteiths equation is the best ( $R^2$  value 0.94 and 0.92 for both semi-arid and sub-humid agroclimates respectively). The Thornthwaite equation has the next highest  $R^2$  value of 0.90 in Semi- Arid climate. The Hargreaves equation has the next highest  $R^2$  value of 0.90 in Sub-Humid climate.

**4.8 Recalibrated crop coefficient (kc):**

Using the crop coefficients mentioned above shows results with 5 to 20 % errors. These errors are due to the changes in the climatological parameters and hence the crop coefficients need to be recalibrated using the formula:

$$k_c = \frac{ET_c}{ET_o} \tag{10}$$

Where,  $ET_c$ : Actual Evapotranspiration measured by lysimeter and  $ET_o$ : Reference Evapotranspiration evaluated by empirical formulae's.

**TABLE 5  
RECALIBRATED CROP COEFFICIENTS FOR THE EMPIRICAL EQUATIONS IN SEMI-ARID AGRO CLIMATE**

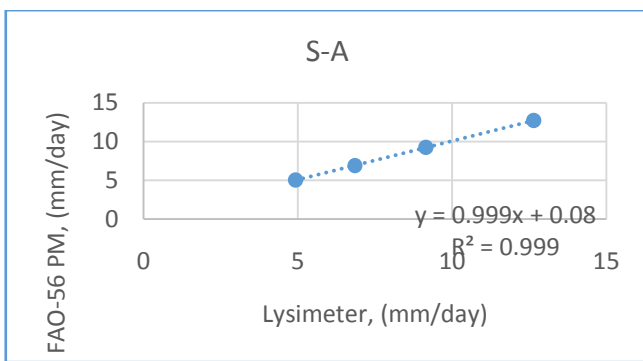
Month	Crop Stage	FAO-56 Penman Monteith	Thornthwaite	BlaneyCriddle	Hargreaves & Samani	Priestly & Taylor	Makkink	Avg. Kc
Mar	Initial	0.71	0.86	0.8	0.86	0.74	0.92	0.78
Apr	Development	0.86	1.23	1.09	1.03	0.99	1.24	1.045
May	Mid	1.56	2.35	1.99	2.27	1.72	2.33	1.95
Jun	Late	1.30	1.78	1.45	2.11	1.21	1.75	1.54

**TABLE 6**  
**RECALIBRATED CROP COEFFICIENTS FOR THE EMPIRICAL EQUATIONS IN SUB-HUMID AGRO CLIMATE.**

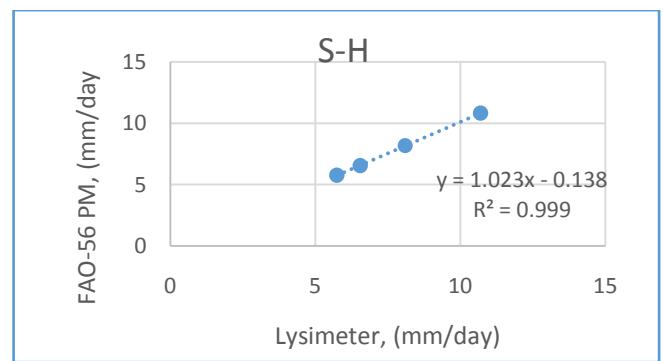
Month	Crop Stages	FAO-56 Penman Monteith	Thornthwaite	BlaneyCriddle	Hargreaves & Samani	Priestly & Taylor	Makkink	Avg
Mar	Initial	0.85	1.18	1.01	0.95	0.879	1.09	0.9
Apr	development	0.91	1.28	1.13	1.05	0.94	1.20	0.98
May	Mid	1.42	2.08	1.85	1.68	1.51	1.97	1.55
Jun	Late	1.27	1.78	1.48	1.33	1.15	1.56	1.55

Table 5 and 6 include the Kc values recalibrated for both the agro climates. Using these crop coefficients the new Actual evapotranspiration rates are evaluated which results less errors when compared with the actual evapotranspiration rates by lysimeter. The mean monthly and seasonal (March- June) values calculated by these equations with the calibrated Kc values. For illustrative purposes the same regression analysis was carried out for the monthly values of evapotranspiration and the results are plotted in Figure 6.

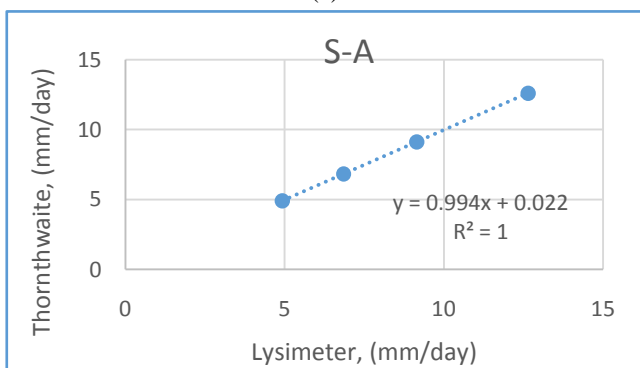
**4.9 Regression Analysis using Recalibrated Crop Coefficients:**



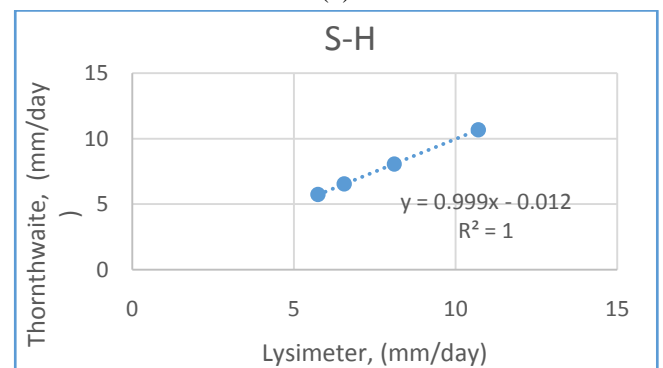
(a)



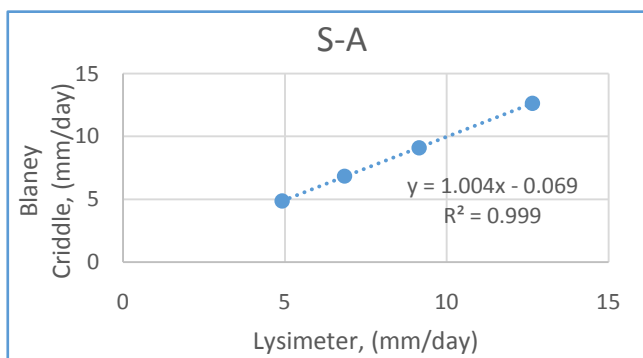
(b)



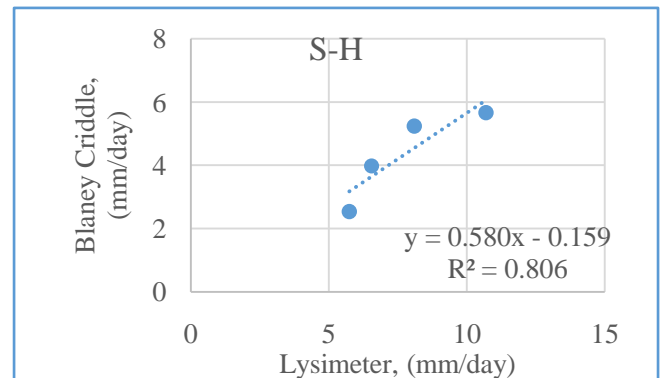
(c)



(d)



(e)



(f)

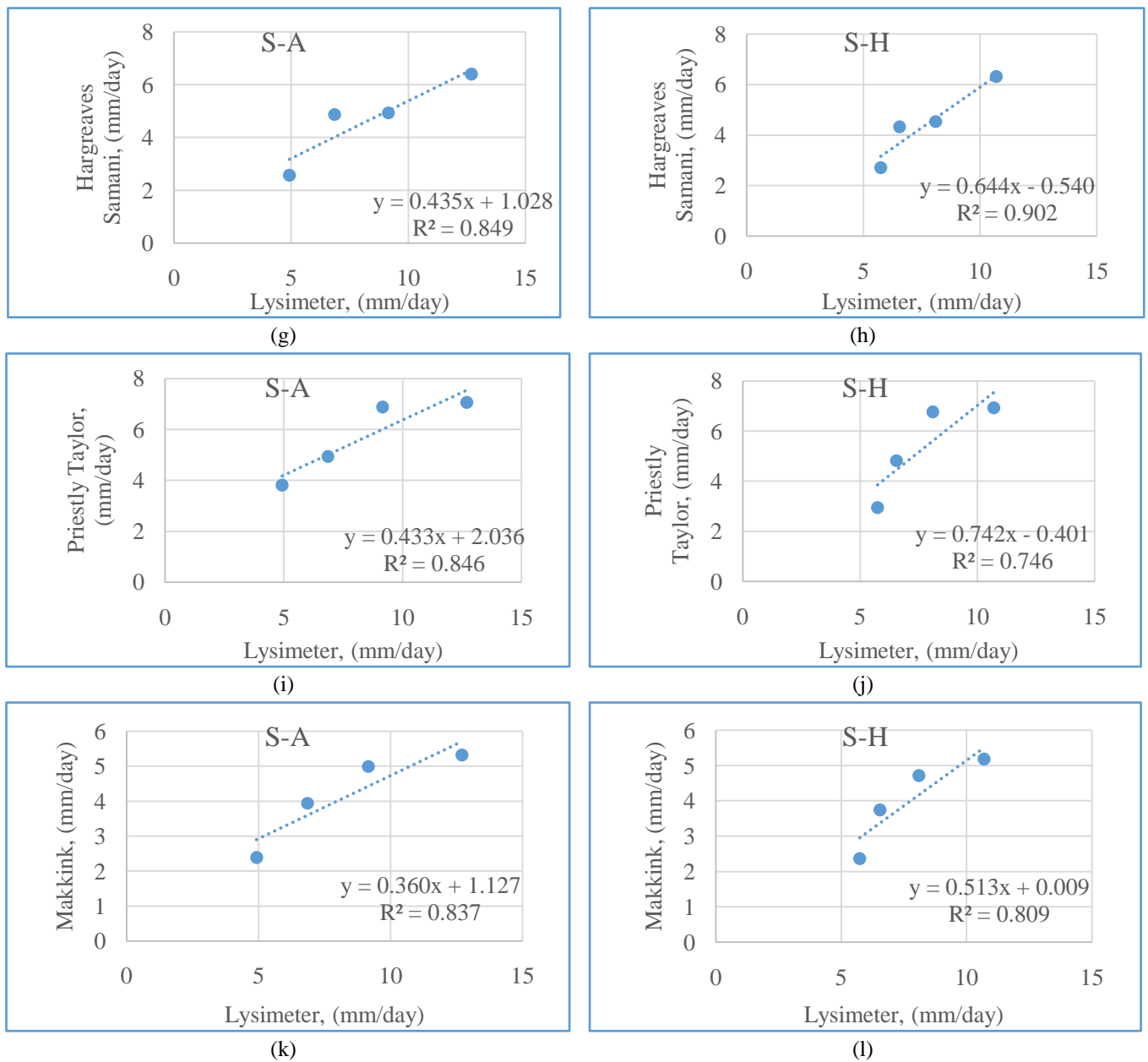


**FIGURE 6: Regression plots for Actual evapotranspiration rates using recalibrated crop coefficients**

(Note:- S-A: Semi-Arid, S-H: Sub-Humid, Fig (a & b): FAO-56 Penman Monteith method, Fig (c & d): Thornthwaite method, Fig (e & f): Blaney Criddle method, Fig (g & h): Hargreaves and Samani Method, Fig (i & j): Priestly and Taylor method, Fig (k & l): Makkink method).

**TABLE 7**

**PERCENTAGE ERRORS BY ORIGINAL KC AND RECALIBRATED KC VALUES FOR SEMI-ARID AGRO CLIMATE**

Methods	Original Kc	%Error	RecaliberatedKc	P
	(mm/day)	(%)	(mm/day)	(%)
FAO-56 PM	6.08	27.46	8.46	0.89*
Thornthwaite	5.055	39.76	8.36	0.29*
BlaneyCriddle	4.735	43.58	8.35	0.41*
Hargreaves &Samani	4.6925	44.08	8.49	1.25**
Priestly & Taylor	5.6775	32.35	8.4	0.12*
Makkink	4.16	50.43	8.38	0.06*

The presented simulation-based continuous Kc curves could support an objective and justifies that there is low water consumption at the initial growth stages of the crop and thereby gradually increases for development stage of the crop and reaches to a maximum level at the mid stage and later gradually tends to fall down at the late stages of the crop. Site-specific irrigation scheduling on a daily basis. The evaluation and comparison were made based on both the original constant values involved in each equation and the recalibrated Kc values. In case of using original Kc values of the six original equations evaluated, the FAO-56 Penman Monteith equation resulted in mean seasonal evapotranspiration values that agreed most closely with lysimeter evapotranspiration values, next to FAO-56 Penman Monteith's Equation Thornthwaite and Hargreaves Samani Equation values were most close to lysimeter values.

**TABLE 8**  
**PERCENTAGE ERRORS BY ORIGINAL Kc AND RECALIBRATED Kc VALUES FOR SUB-HUMID AGRO CLIMATE**

Methods	Original Kc	%Error	Recalibrated Kc	P
	(mm/day)	(%)	(mm/day)	(%)
FAO-56 PM	5.83	24.96	7.815	0.54*
Thornthwaite	3.79	51.22	7.75	0.22*
Blaney Criddle	4.35	44.01	7.74	0.32*
Hargreaves & Samani	4.47	42.47	7.86	1.12**
Priestly & Taylor	5.37	30.88	7.79	0.28*
Makkink	3.99	48.64	7.74	0.32*

(Note: \*\*  $P < 0.05$ , \*  $P < 0.01$ )

## V. IMPACT ON CROP WATER REQUIREMENT

Irrigation requirements are developed with the help of crop water requirement of every crop. Hence for designing the irrigation system Evaluation of ET rates are very essential. For a typical tomato crop, while designing the crop water requirement this study provides proper crop coefficient values that can be used for evaluating the actual evapotranspiration rates. We can see that there are about 5% to 20% errors occurred by using the original Kc values as given by Rowell and Soe, 2016. Therefore, after recalibrating the crop coefficients the same models provided good results hence using these recalibrated crop coefficients provide goods results with less errors about 0.06% - 1.25 % (Table 7). In designing the crop water requirement now using these crop coefficients for determining the consumptive use of a tomato crop results more accurate requirement. Crop coefficient does not only vary with climate but in combination with crop stage. Irrigation frequency and water supply for each watering depends on crop stage besides evapotranspiration rates, thus crop coefficients are to be computed in combination with climate parameters as well as crop stage.

## VI. CONCLUSION

Irrigation requirements are developed with the help of crop water requirement of every crop. Hence for designing the irrigation system Evaluation of ET rates are very essential. Actual Evapotranspiration using various Empirical methods and field experiments by lysimeters and recalibrating the crop coefficients for different agro climates and upcoming with the suitable method for computation of Evapotranspiration rates for the respective climates. The average Actual ET for tomato crop by lysimeter method for Semi-Arid region was estimated to be 8.39 mm/day and in Sub-Humid region it was about 7.77 mm/day and therefore the corresponding correlations with FAO-56 PM equation was found to be 0.94 for Semi-Arid region and 0.92 for Sub-Humid region. Thornthwaite equation when correlated with the lysimeter gave a value of 0.9 and therefore is next well suited method for computing ET in semi arid region. In the same way Hargreaves Samani Equation correlated well with a value of about 0.9 and hence is the next well suited method in Sub Humid region. Due to large climatological data requirement by FAO-56 PM equation it becomes non feasible for estimation ET though it gives accurate results, But in some areas climate data are not available, there this method is difficult to carry out. Together with weather forecasts of rain and evapotranspiration for the next days, such a simulation model platform could be part of a decision support system on crop irrigation. In a next step, the simulated Kc curves could be generated and mapped for other field crops and for relevant agronomic regions including applications with national and global data sets with noticeably differing weather conditions including gridded weather data.

## ACKNOWLEDGEMENTS

The authors would especially like to thank the farmers for their cooperation and support in carrying out the project in their fields. The authors wish to acknowledge the Karnataka State Natural Disaster Monitoring Center for providing weather data

needed for this study. The scholar expresses his thankfulness to Librarians of UBTD college of Engineering Library, Davanagere; for their help rendered to her in providing relevant books, journals and data concerning my research study. The scholar also submits all her praise and thanks to her loved ones i.e., Parents and friends from the depth of heart for their blessings and helping in all aspects of life and the research work.

## REFERENCES

- [1] Ariel Dinar, Amanda Tieu and Helen Huynh (2019), “*Water scarcity impacts on global and food production*”, Global Food Security, Vol 23, 212-226.
- [2] Brent Rowell and Mar LarSoe (2016), “*Simplified Water Requirement Calculators for Fruits and Vegetables*”, HoriTechnology, 26(4).
- [3] C. H. B. Priestley and r. J. Taylor (1972), “*On the assessment of surface heat flux and evaporation using large-scale parameters*”, monthly weather review, vol. 100, no. 2, 81-91.
- [4] C. Y. Xu and V. P. Singh (2002), “*Evaluation and Generalization of Temperature-based methods for calculating evaporation*”, Hydrological Processes, **15**, 305-319.
- [5] Daniel K. Fisher and H. C. Pringle III (2013), “*Evaluation of alternative methods for estimating reference evapotranspiration*”, Agricultural Sciences, Vol.4, No.8A, 51-60.
- [6] DanluGuo, Seth Westra, Holger R. Maier (2016), “*An R package for modelling actual, potential and reference evapotranspiration*”, Environmental Modelling & Software 78, 216-224.
- [7] George H. Hargreaves, Zohrab A. Samani (1985), “*Reference Crop Evapotranspiration from Temperature*”, American Society of Agricultural Engineers, Vol 1(2), 0883-8542.
- [8] George P. Petropoulos, Prashant K. Srivastava, Maria Piles and Simon Pearson (2018), “*Earth Observation-Based Operational Estimation of Soil Moisture and Evapotranspiration for Agricultural Crops in Support of Sustainable Water Management*”, Sustainability, 10, 181; doi:10.3390/su10010181.
- [9] G. Nanjundan, Nanjundappa GariKeerthy\* and Sadiq Pasha (2019), “*Rainfall Trend Analysis for Karnataka State with Spatial Distribution*”, Journal of Computer and Mathematical Sciences, Vol.10 (6), 1236-1243.
- [10] GOI (2016) Manual for drought management. Department of Agriculture, Cooperation & Farmers Welfare Ministry of Agriculture & Farmers Welfare, Government of India, New Delhi
- [11] HARRY F. BLANEY and WAYNE D. CRIDDLE (1962), “*Determining Consumptive Use And Irrigation Water Requirements*”, Agricultural Research Service UNITED STATES DEPARTMENT OF AGRICULTURE
- [12] Intergovernmental Panel on Climate Change (IPCC) (2014) Climate change 2014: impacts, adaptation, and vulnerability. Cambridge University Press, New York
- [13] J. doorenbos and W. O. Pruitt (1977), “*Guidelines for Predicting Crop Water Requirements*”, FAO Irrigation and Drainage paper
- [14] Jianping Huang, Mingxia Ji, Yongkun Xie, Shanshan Wang, Yongli He and Jinjiang Ran (2016), “*Global semi- arid climate change over last 60 years*”, open access at Springerlink, 46:1131-1150.
- [15] K. Djaman and S. Irmak, M. ASCE (2013), “*Actual Crop Evapotranspiration and Alfalfa- and Grass-Reference Crop Coefficients of Maize under Full and Limited Irrigation and Rainfed Conditions*”, Journal of Irrigation and Drainage Engineering, Vol. 139, No. 6, 433-446.
- [16] Koffi Djaman, Alpha B. Balde, Abdoulaye Sow, Bertrand Muller, Suat Irmak, Mamadou K. N’Diaye, Baboucar Manneh, Yonnelle D. Moukoubi, Koichi Futakuchi and Kazuki Saito (2015), “*Evaluation of sixteen reference evapotranspiration methods under sahelian conditions in the Senegal River Valley*”, Journal of Hydrology: Regional Studies 3 139-159.
- [17] Lakshman Nandagiri and Gicy M. Kovoov (2006), “*Performance Evaluation of Reference Evapotranspiration Equations across a Range of Indian Climates*”, Journal of Irrigation and Drainage Engineering, 132:238-249.
- [18] Nithya Rajan (2007), “*Estimation of Crop Water Use for Different Cropping Systems in the Texas High Plains Using Remote Sensing*”, A Dissertation In Agronomy,
- [19] P.R. Anjitha Krishna (2019), “*Evapotranspiration and agriculture-A review*”, Agricultural Research Communication Centre, Agricultural Reviews, 40(1) 2019: 1-11.
- [20] P. Ravikumar, R. K. Somashekar and Mhasizonuo Angami (2011), “*Hydrochemistry and evaluation of groundwater suitability for irrigation and drinking purposes in the Markandeya River basin, Belgaum District, Karnataka State, India*”, Environ Monit Assess, 173:459-487. DOI 10.1007/s10661-010-1399-2.
- [21] Richard G. Allen, Luis S. Pereira, Dirk Raes, Martin Smith (1998), “*Crop evapotranspiration - Guidelines for computing crop water requirements*”, FAO Irrigation and drainage paper 56.
- [22] Thornthwaite, C. W (1948), “*An Approach toward a Rational Classification of Climate.*” Geographical Review, vol. 38, no. 1, pp. 55-94.
- [23] U. Surendran, B. Anagha, P. Raja, V. Kumar, K. Rajan & M. Jayakumar (2019), “*Analysis of Drought from Humid, Semi-Arid and Arid Regions of India Using DrinC Model with Different Drought Indices*”, Water Resources Management, DOI: 10.1007/s11269-019-2188-5.
- [24] Y. Dinpashoh, S. Jahanbakhsh-Asl, A. A. Rasouli, M. Foroughi and V. P. Singh (2018), “*Impact of climate change on potential evapotranspiration (case study: west and NW of Iran)*”, Theoretical and Applied Climatology, doi: 10.1007/s00704-018-2462-0.
- [25] S.J. Seidel, K. Barfus, T. Gaiser, T.H. Nguyen and N. Lazarovitch (2019), “*The influence of climate variability, soil and sowing date on simulation-based crop coefficient curves and irrigation water demand*”, Agricultural Water Management 221, 73-83.

# Heat Transfer and Unsaturated Flow Phenomena in Rigid Dual-Scale Porous Media

Nirmal Kumar Balaguru<sup>1</sup>, M. Jeyameena<sup>2</sup>

<sup>1</sup>Development Engineer, Kraft Recovery Boilers (R&D), Andritz paper and pulp

<sup>2</sup>Student, Hindusthan College of Engineering and Technology, Coimbatore

**Abstract**— Composites are light weighted materials that can replace the metals in strength promisingly in future. The residual porosity of the composites alters the thermo-physical properties of the material to a maximum level. During the impregnation of fibre in matrix (injection), the presence of air voids changes the direction of the flow of resin. This also affects the material properties in terms of flexibility, durability but agitates the effective thermal conductivity ( $k_{eff}$ ). The physics behind the effect of air void on the effective thermal conductivity cannot be captured in commercial software or experiments. The best way to solve this problem is by numerical codes using finite element approach, by dividing the whole macroscopic domain into numerous subdomains as possible. The divided subdomain should be periodic in nature with respect to the whole domain. If the heterogeneities are similar, dual scale approach is used and so on. If the heterogeneities are different and if they are of two types, triple scale approach is used. The contrast ratio and volume percentage of fiber is used as variables. The air void creates a giant leap for saturation in both, which in turn effect the effective thermal conductivity. Air void troubles the effective thermal conductivity mainly because of its insignificance in scalar values of thermal conductivity when it is compared to fiber or matrix mathematically.

**Keywords**— composites, effective thermal conductivity, homogenization, impregnation, matrix, fibre, preform, contrast ratio, saturation, liquid composite moulding.

## I. INTRODUCTION

The Liquid Composite moulding (LCM) is one of the most predominant processes in the manufacturing of composites. The reinforcement of dry fiber called as preform is kept inside the moulding cavity. The moulding cavity is locked and the resin is injected to the moulding cavity. Initially, the resin that is injected to moulding cavity will rush the air entrapped between the fibrous networks outside the moulding cavity thus forming a composite on curing.

The major defect during injection is voids, These are due to entrapment of dissolved volatile gases in resin or due to improper balance of velocity and capillary force. There are voids formed within the tows and also in between the tows, naming micro porosity and macro porosity respectively. As described by R.J Bascom [1], the composite test rings having void contents of 0.2 Volume % or less had interlaminar shear strengths 40-100% greater than the conventional rings with high void contents(5%). The void formation is related to the liquid properties and fluid-liquid contact angle. The micro scale flow pattern and the void formation, movement and removal is related to fibre mat architecture [7].

The laminates with the highest average content of voids had an transverse strain to failure as high as 2% whereas low void content laminates failed at 0.3%. Low void content laminates form only few large and well defined transverse cracks whereas the high void content laminates form multiple transverse cracks with irregular shapes and also small cracks. The irregularity of these cracks results in lower stress concentration as per the conclusion of J.Vama [2].

The LCM processes such as Resin transfer moulding is increasingly used to manufacture parts of industrial application and were cost efficient. The work by LS Lecrec [5] which was carried out on different type of fibrous reinforcements and the optimal condition for the impregnation of resin to avoid macro and micro voids relating the local capillary number. The contrasts in the thermal properties existing between the dry and the fully saturated reinforcement is used to determine the dynamic saturation curve. As explained by Maxime Viliere [6] the evolution of residual voids for several resin flow rates with respect to the capillary number.

When the material properties of the composites are known the effective thermal conductivities of woven-reinforcement composites is predicted the models proposed by Maxime Villiere [9]. The heterogeneous media uses two pairs of local and

homogenized problems, described at the smallest scale is seen to affect the medium macro-scale or effective behaviour. The homogenization is used to formulate the Fourier heat conduction problem[10].The homogenization process using the double scale asymptotic developments as macroscale and microscale is much appropriate[11] and it also permits the determination of the correct model for a given macroscopic boundary value [12].

## II. METHODOLOGY

### 2.1 Homogenization

This process can be defined as the converting the domain with numerous heterogeneities to homogeneous domain. It is a process in which the heterogeneities in a domain are divided into small subdomain. This process can be defined as the converting the domain with numerous heterogeneities to equivalent homogeneous domain. Consider heat equation,

$$\rho C_p \frac{\partial T}{\partial t} + \text{div} \cdot (K \cdot \nabla T) = 0 \tag{1}$$

Assuming it as steady heat flux,

$$\text{div} (-\varphi) = 0 \tag{2}$$

Where  $\varphi$  is the heat flux density

$$\varphi = K \cdot \nabla T \tag{3}$$

The version of homogenised equation can be written as

$$\langle \varphi \rangle = \langle \varphi(X) \cdot \nabla T(X) \rangle = K^* \cdot \langle \nabla T \rangle \tag{4}$$

Where  $k^*$  is known as effective thermal conductivity in macroscopic scale. We can see how the conductivity in the micro scale is homogenised to macro scale through the process of homogenisation.

#### 2.1.1 Analytical Method

Consider a domain  $\Omega$ , having the boundary  $\partial\Omega$ . The microscopic domain surfaces are periodic which means that the same domain can be repeated numerous times as required. The borders of the domain are having the temperature of  $T^0$ .

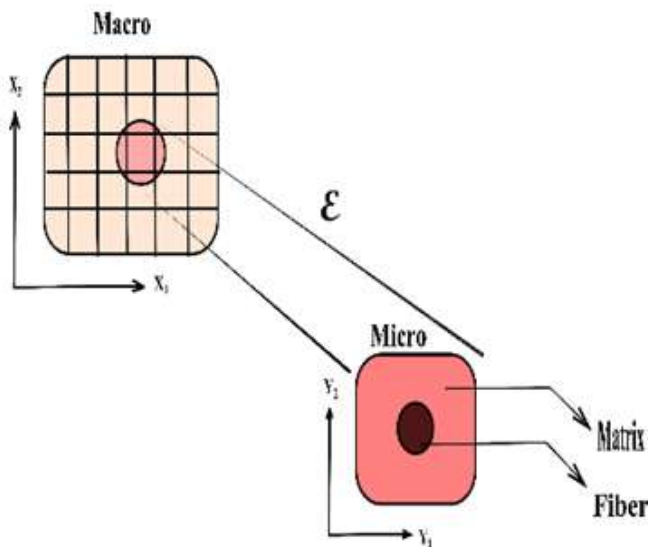


FIG 1: Physical way of Homogenization

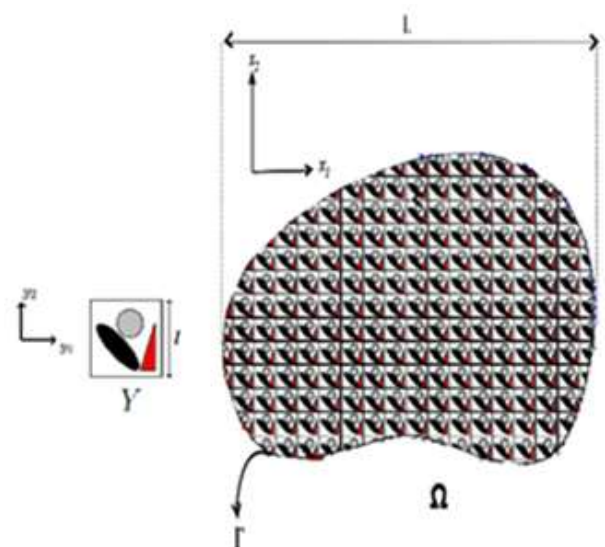


FIG 2: Micro and Macro cells

$$\text{div}_X (-\varphi^\varepsilon(X)) = f(x) \quad \text{in } \Omega \tag{5}$$

$$\varphi^\varepsilon(X) = K \cdot \nabla_X T^\varepsilon(X) \quad \text{in } \Omega \tag{6}$$

$$T = T^0 \quad \text{on } F \tag{7}$$



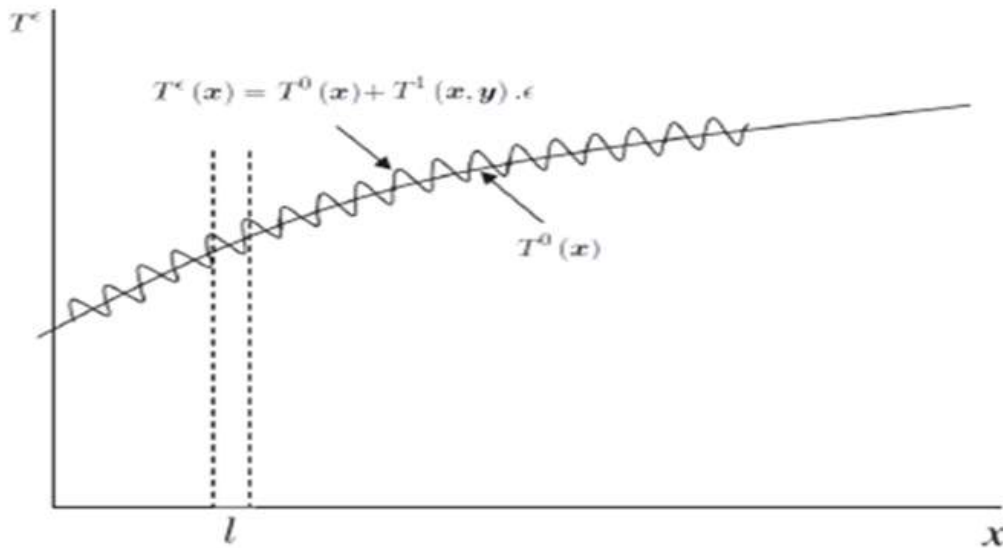


**FIG 3: Asymptotical approach**

To determine the asymptotic behaviour of the temperature  $T$  and flux  $\phi$ , solutions of the heterogeneous problem arises when  $\epsilon$  tends to 0 when we use here the method asymptotic developments several scales. This is done by expanding  $T$  by the following development.

$$T^\epsilon(x, y) = T^0(x, y) + \epsilon T^1 + \epsilon^2 T^2 + .. \tag{8}$$

$$\phi^\epsilon(x, y) = \phi^0(x, y) + \epsilon \phi^1 + \epsilon^2 \phi^2 + ... \tag{9}$$

Divergence between macro and micro scales can be derived as,

$$\nabla = \frac{\partial}{\partial x} + \frac{1}{\epsilon} + \frac{\partial}{\partial y} \tag{10}$$

When the divergence are expanded in heat equation for  $k$ ,  $T$  and  $T$  is expanded asymptotically, Steady state heat conduction equation

$$\nabla \cdot (K \nabla T) = 0 \tag{11}$$

solving for  $\epsilon^{-2}$  problem it leads to,  $T^0 \rightarrow T(x)$  only Hence  $T^0$  can be only used for macroscale.

solving for  $\epsilon^{-1}$  problem it leads to,

$$T^1(x, y) = W \cdot \nabla \cdot T^0 \tag{12}$$

And also the cell equation

$$\nabla_y \cdot (K (e_i + \nabla_y W_i)) = 0 \tag{13}$$

Solving for  $\epsilon^0$  problem it leads to,

$$\nabla_x \cdot \left[ \frac{1}{|P|} \int_p K (I + \nabla_y W(y)) \right] \nabla_x T^0 = 0 \tag{14}$$

And

$$K^* = \frac{1}{|P|} \int_p K (I + \nabla_y W(y)) \tag{15}$$

such that

$$\nabla K \nabla T = 0$$

2.1.2 Numerical Analysis

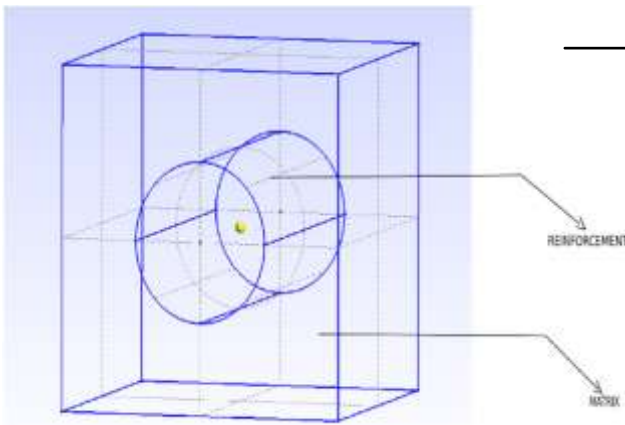


FIG 4: Type 1 cell – fiber at centre alone

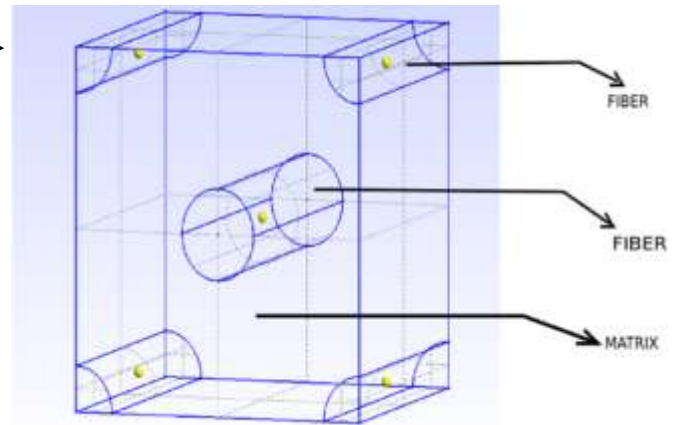


FIG 5: Type 2 cell – fiber at centre and at corner

The unit cell geometry is created by having fiber at centre alone and fiber with centre and at corner also. Since, it is a unit cell the cube is of dimensions 1 x 1 x 1. The Grid independence study has been carried out for three different characteristic length and the  $k_{eff}$  has found the minimum change between the two types.

The characteristic element doesn't have any length since, it is dimensionless. Gmsh software is used to generate the geometry and mesh and the Free Fem++ is used to solve the problem.

	COARSE	FINE	SUPER-FINE
VERTICES	1237	10081	69481
TETRAHEDRONS	4672	54272	384176
TRIANGLES	1728	4096	15384
No of ELEMENTS	6400	58368	350560

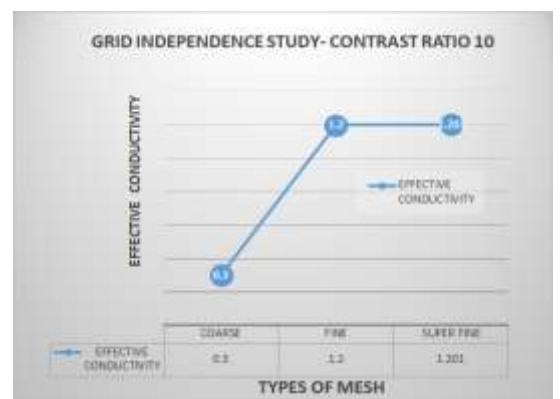


FIG 6 & 7: Grid Independence study

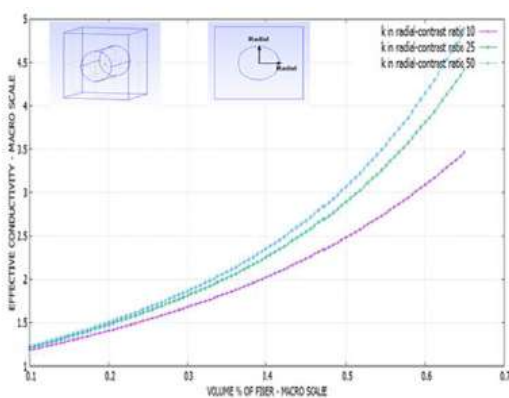


FIG 8: The evolution of  $k_{eff}$  at macroscale in radial direction with different C.R

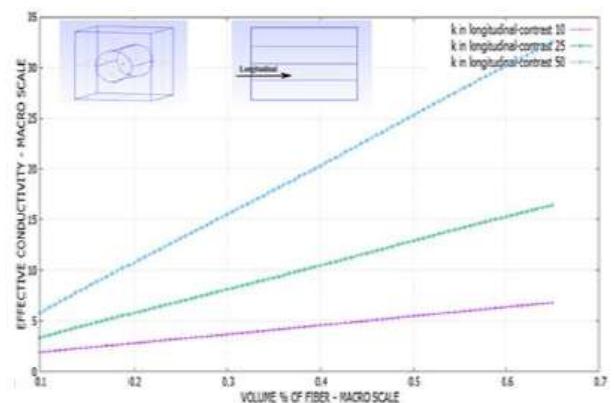


FIG 9: The evolution of  $k_{eff}$  at macroscale in longitudinal direction with different C.R.

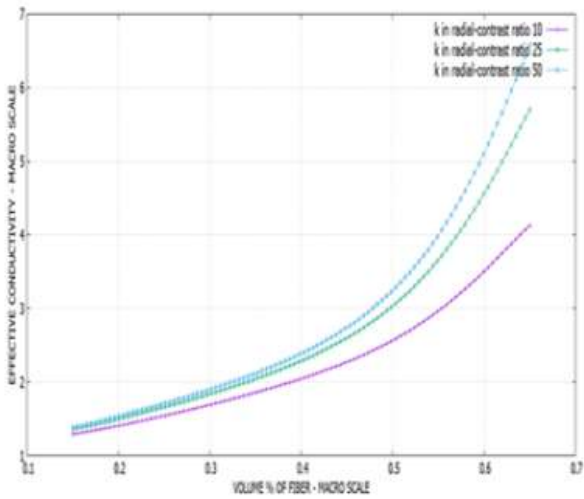


FIG 10: The evolution of  $k_{eff}$  at macroscale in radial direction with different C.R – Type 2 cell

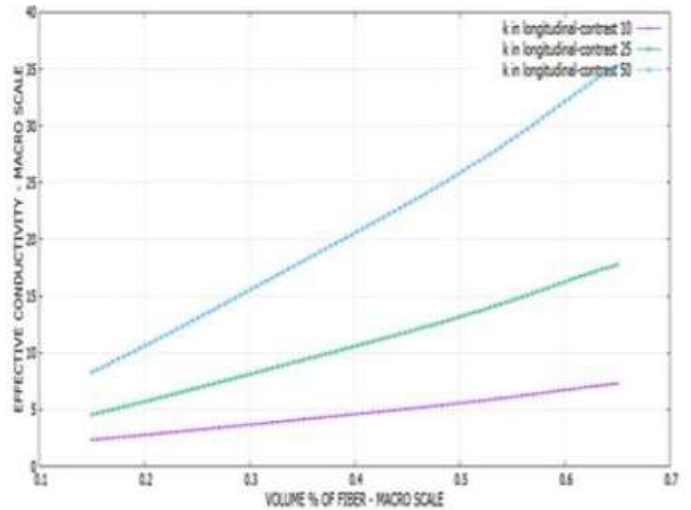


FIG 11: The evolution of  $k_{eff}$  at macroscale in longitudinal direction with different C.R – Type 2 cell

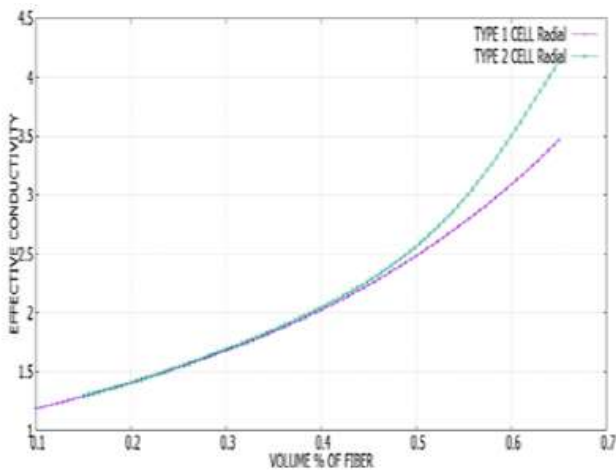


FIG 12: Type 1 Vs Type 2 cell in radial direction for contrast ratio 10

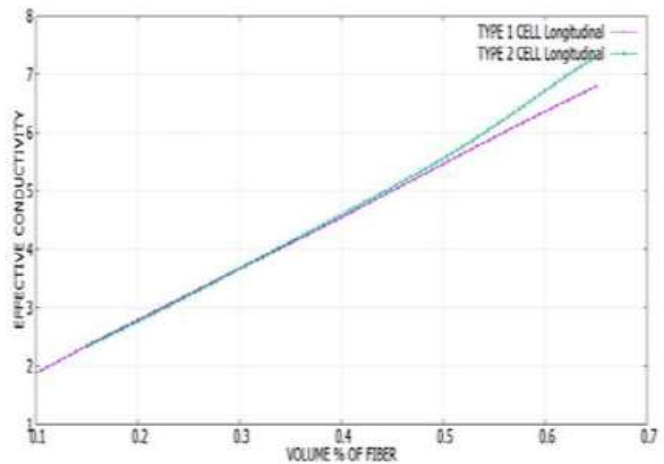


FIG 13: Type 1 Vs Type 2 cell in longitudinal direction for contrast ratio 10

2.2 Triple Scale

In the iterative homogenization, the homogenization is done multiple times in which the solution of microscopic scale to mesoscopic tows are taken. On preceding the next step of homogenization the macroscopic properties are obtained.

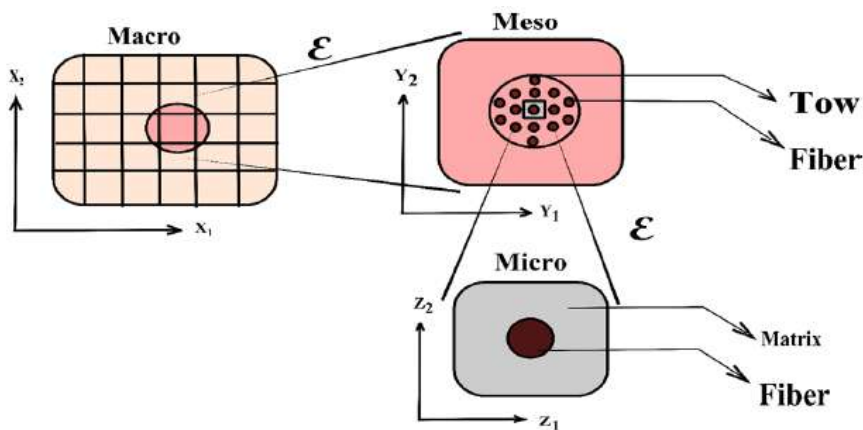


FIG 14: Iterative Homogenisation

### 2.2.1 Analytical Analysis

If the heterogeneities are in dual scale, homogenisation is done in iterative manner. This can be considered as a realistic approach.

The macro, meso and micro scale is taken as x, y and z scale respectively. The divergence in x,y,z scales are differentiated as,

$$\nabla_x = \begin{pmatrix} \frac{\partial}{\partial x_1} \\ \frac{\partial}{\partial x_2} \\ \frac{\partial}{\partial x_3} \end{pmatrix} \quad \nabla_y = \begin{pmatrix} \frac{\partial}{\partial y_1} \\ \frac{\partial}{\partial y_2} \\ \frac{\partial}{\partial y_3} \end{pmatrix} \quad \nabla_z = \begin{pmatrix} \frac{\partial}{\partial z_1} \\ \frac{\partial}{\partial z_2} \\ \frac{\partial}{\partial z_3} \end{pmatrix} \quad (17)$$

The calculation can be done with

$$\nabla = \frac{\partial}{\partial x} + \frac{1}{\varepsilon} \frac{\partial}{\partial y} + \frac{1}{\varepsilon^2} \frac{\partial}{\partial z} \quad (18)$$

When this is substituted to heat equation,

$$\nabla \cdot (K \nabla T) = 0 \quad (19)$$

The equations which we obtain are similar, but the only difference is calculation is carried in two steps. Micro meso is one step and meso macro is another step.

As a first step let us explain  $T^\varepsilon$

$$T^\varepsilon(x, y) = T^0(x, y) + \varepsilon T^1 + \varepsilon^2 T^2 + \dots \quad (20)$$

The divergence between meso and micro scales can be declared as

$$\nabla = \frac{\partial}{\partial y} + \frac{1}{\varepsilon} \frac{\partial}{\partial z} \quad (21)$$

When it is solved for  $\nabla k \nabla T$ , by taking mean and applying greens theorem for order -2 we will get to know that  $T^0$  is a macroscopic property

When we solve the order of -1 we will get cell equation as,

$$\nabla_z (k(e_i + \nabla_z W_i)) = 0 \quad (22)$$

And also the same order of scaling factor leads to

$$T^1 \rightarrow T^1(x, y) = X(y) \cdot \nabla_x T^0 \quad (23)$$

The effective conductivity in radial and longitudinal direction for micro scale is found using the following equation. These values are substituted to effective conductivities for meso scale and so the macro properties are found

$$k^* = \frac{1}{|P|} \int_P k(I + \nabla_y W(y)) dp \quad (24)$$

The same procedure has to be carried out for the meso macro where the macro properties are found

$$k^* = \frac{1}{|P|} \int_P k(I + \nabla_x X(y)) dp \quad (25)$$

Where P refers to the periodic domain. So the thermal conductivities obtained in this meso scale is considered as the final values for the macro scale.

### 2.2.2 Numerical analysis

**Iterative homogenisation in actual:** The cell geometry used for microscopic scale and mesoscopic scale should be different. The double homogenisation method should be more realistic. An elliptical geometry is considered in mesoscopic scale and the similar cylinder geometry is carried out for microscopic scale. This is a true approach and can be used for better accuracy. The microscopic heterogeneities repeat periodically in mesoscopic scale and mesoscopic heterogeneities are repeating periodically in macroscopic scale.

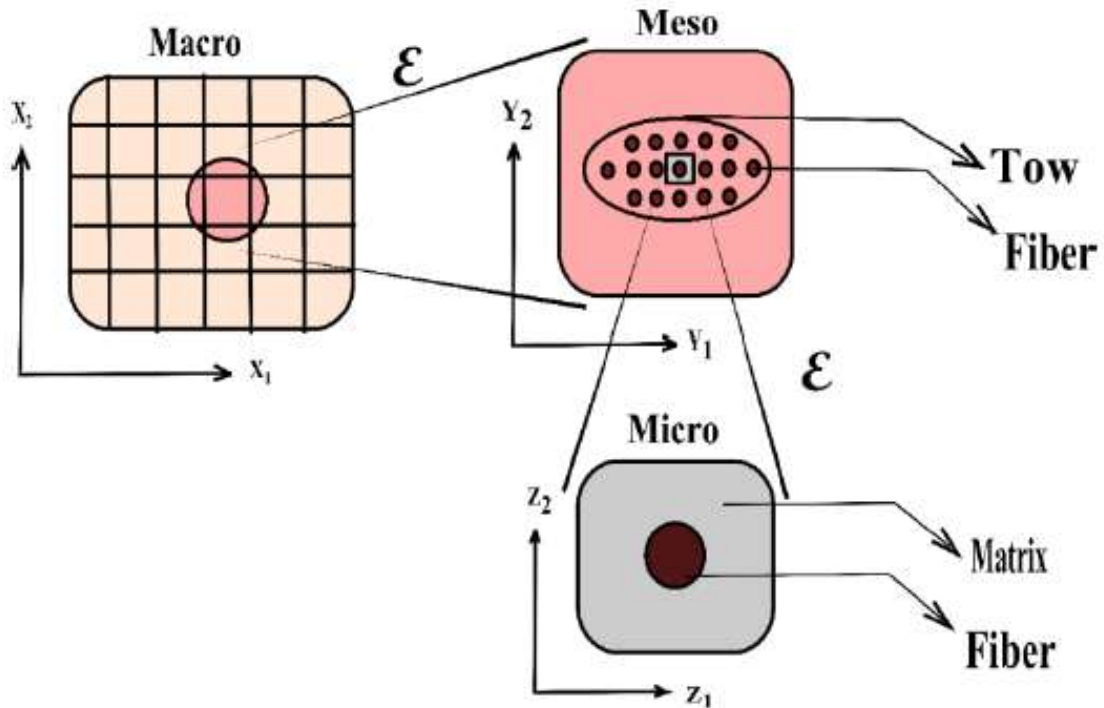


**FIG 15: Physical explanation for actual way to do double**

This is done using software as follows when we implement to the unit cell with fibre in centre alone.

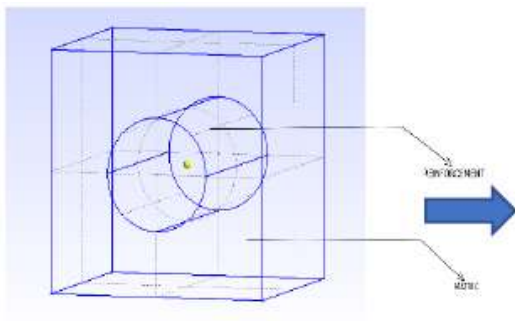


**FIG 16: Micro cell for actual double homogenisation**

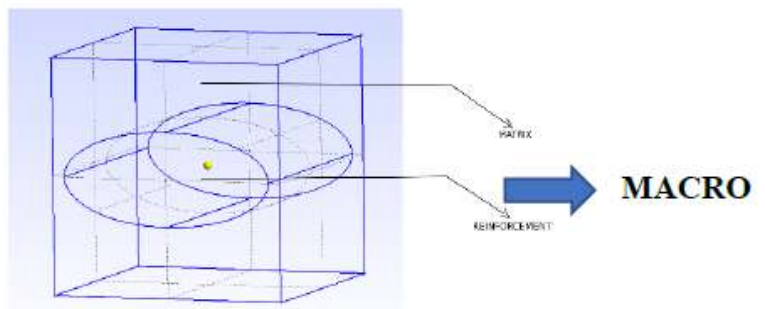


**FIG 17: Meso cell for actual double homogenisation**

The evolution in meso scale

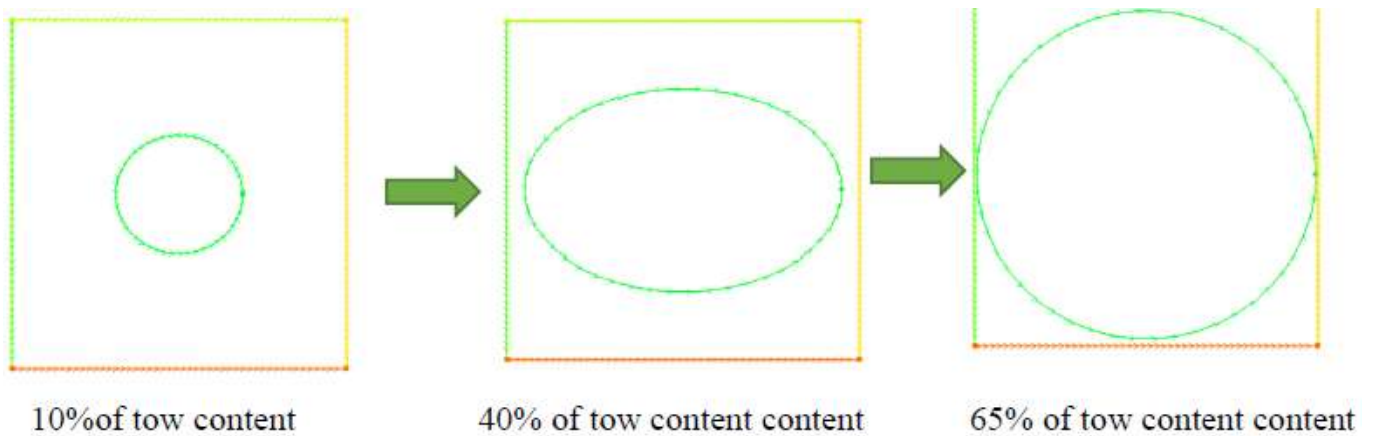


**FIG 18: Evolution of Meso scale**

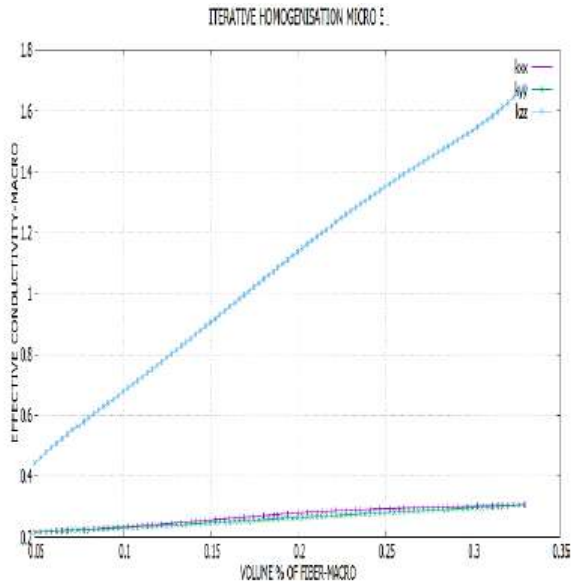


**FIG 19: Effective conductivity in radial and longitudinal direction for volume percentage of fiber in micro scale is fixed to 65**

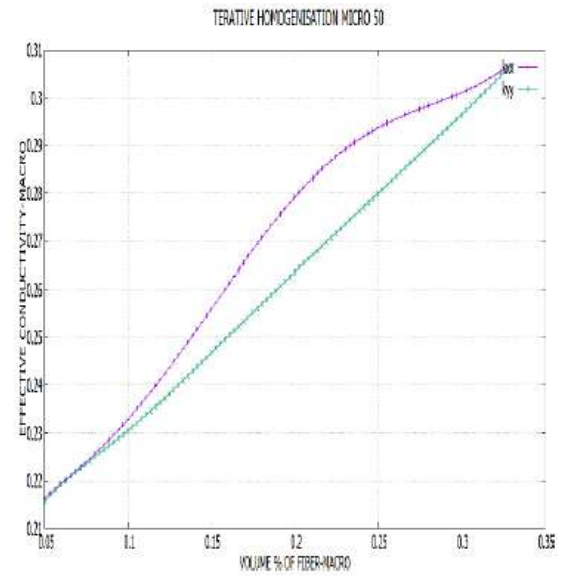


**FIG 20: Zoomed view for plot to explain effective conductivity in radial direction**

When the fiber inside the microscopic unit cell is fixed as 50% for whole cell volume, and if the fiber inside the mesoscopic cell is changed from 10% to 65 % the following plot is obtained. Plots to explain effective conductivity in radial and longitudinal direction for volume percentage of fiber in micro scale is fixed to 65. Zoomed view for plots to explain effective conductivity in radial direction.

**2.3 Saturation**

The voids created in LCM are of different natures depending on whether they are in or between the fibre it can lead to two effects micro-saturation, macro-saturation. The geometric parameters are of the two scales reinforcement. The volume rate of fibres in the composite is noted as  $\phi_f^c$ . The volume percentage of fibre in microscale denoted by  $\phi_f^m$ . The volume fraction in a tow is  $\phi_m^c$ .

Such that

$$\phi_f^c = \phi_f^m * \phi_m^c \tag{2.26}$$

**2.3.1 Micro saturation**

Micro saturation is defined as the space that is present in the cell for the matrix to fill in Micro Scale. Micro-saturation is calculated as followed,

$$S_\mu = 1 - \frac{\text{volume percentage of airvoid in microscale}}{\text{volume percentage of matrix in microscale}}$$

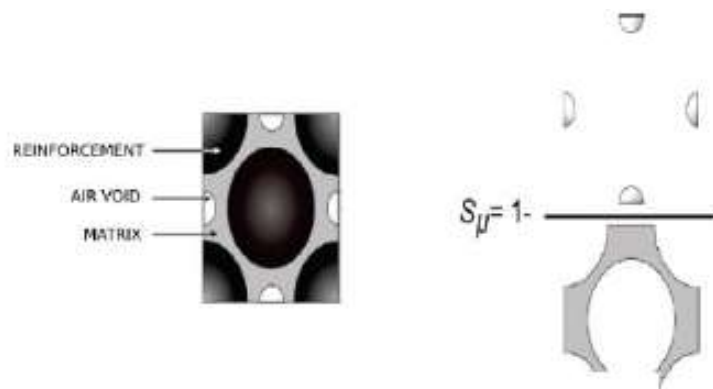


**FIG 21: Micro saturation**

**2.3.2 Micro saturation**

Macro-saturation is defined as the complement of the ratio of the total volume of macro voids subtracted to the total volume they could take maximum, namely the inter-space available other than bubbles.

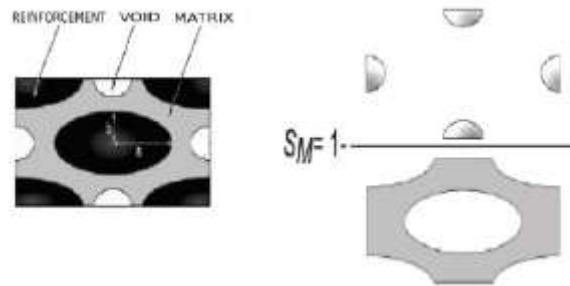


**FIG 22: Meso Saturation**

$$S_M = 1 - \frac{\text{volume percentage of airvoid in macroscale}}{\text{volume percentage of matrix in macroscale}}$$

**2.3.3 Total saturation**

The total saturation or the overall saturation of the reinforcement as a linear combination of micro- and macro-saturations, weighted by factors that depend only on the geometry of the fiber and voids. These reflect the fluid fractions present in the strands and between the strands.

The Total saturation is obtained by

$$S_T = \left( \frac{\varphi_m^c - \varphi_f^c}{1 - \varphi_f^c} \right) S_{\square} + \left( \frac{1 - \varphi_m^c}{1 - \varphi_f^c} \right) S_M \tag{27}$$

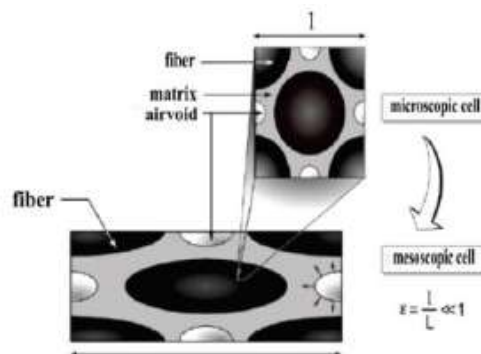


**FIG 23: Iterative homogenization**

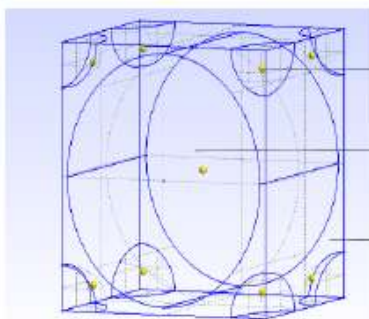


**FIG 24: Micro cell with voids**

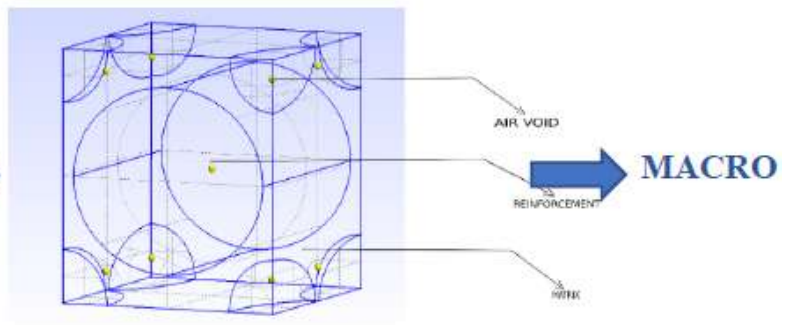


**FIG 25: Meso cell with voids**

Where  $S_M=0$  the curve is obtained, the space intermeches is filled in an ideal manner, the bubbles located only within the stands. The above tells us that the inter-locks space represent 59% of the volume that can occupy the fluid because

$$\left(\frac{1-\varphi_m^c}{1-\varphi_f^c}\right) = 0.59 \tag{28}$$

Calculation of the thermal conductivity was then repeated for all possible pairs of  $S_\mu$ -SM. The curves are set in SM, and for each value of  $S_\mu$ , the ST value is found. The set of curves obtained represents what is referred to hereinafter as a set of curves radial and longitudinal thermal conductivity.

**2.4 Computational method**

The calculations are done by fixing the saturation in meso scale, and changing the saturation value in micro scale from 1 that is known as fully saturated to 0 where only dry air is present.

The values of effective conductivity that are obtained are plotted against the total saturation values

**TABLE 1  
PARAMETERS FOR STUDY SATURATION**

Parameters	Values
$\varphi_m^c$	0.70
$\varphi_f^c$	0.70
$\varphi_f^c$	0.49
rf	0.472
a	0.45
b	0.37

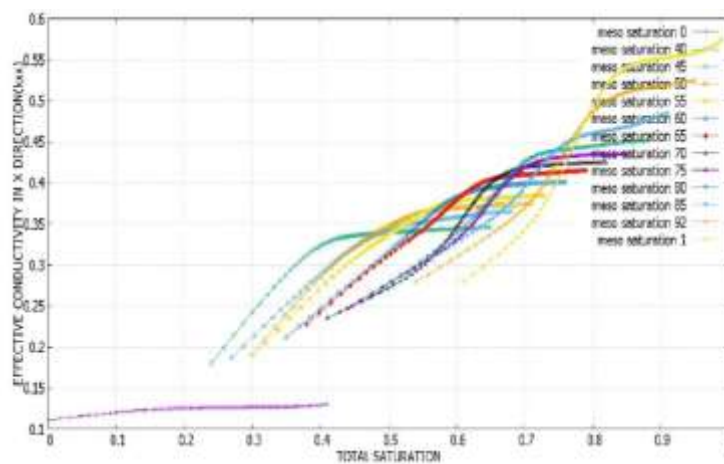


**FIG 26: Plot that explains about variation of effective conductivity in x – direction w.r.t. total saturation**

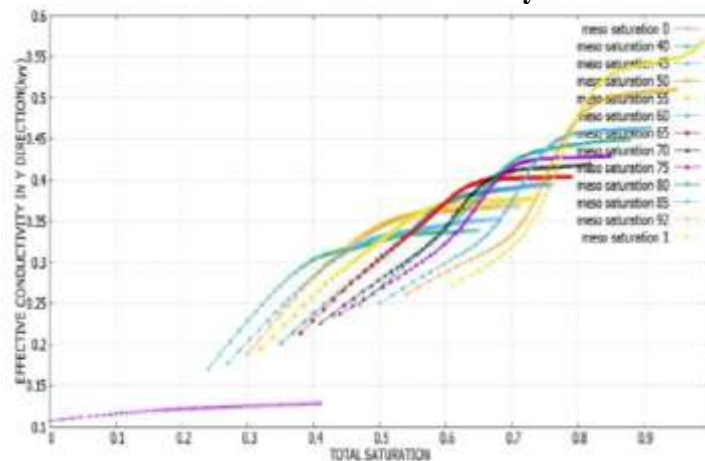


**FIG 27: Plot that explains about variation of effective conductivity in y – direction w.r.t. total saturation**



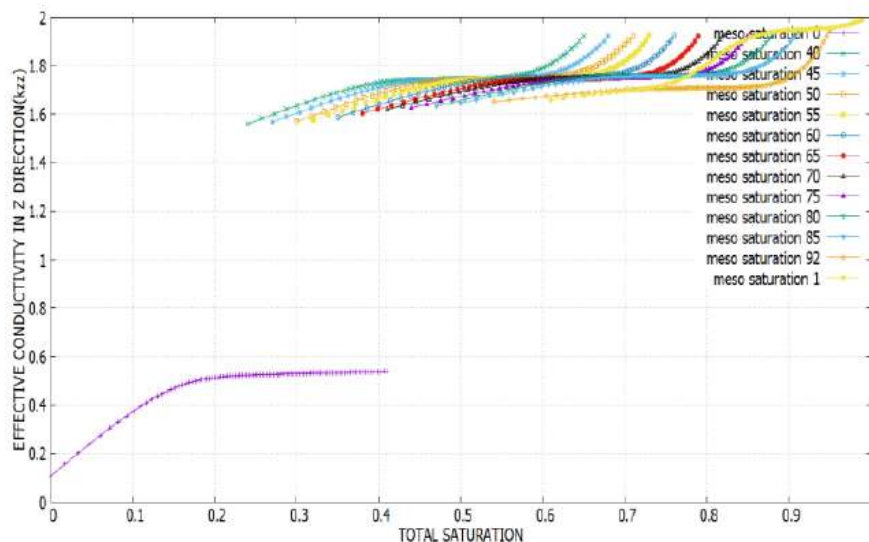


**FIG 28: Plot that explains about variation of effective conductivity in y – direction w.r.t. total saturation**

### III. CONCLUSION

By this research work the following studies had been done.

- The contrast ratio influences effective thermal conductivity. The ratio of thermal conductivity between the fibre and matrix is known as contrast ratio. As this parameter increases the effective thermal conductivity increases drastically.
- The volume percentage of fibre in macro scale can be determined directly by the fibre content in micro scale in dual homogenisation. In iterative homogenisation the volume percentage of fibre in macro scale is determined by fibre content in micro scale and the rate at which fibre is rooved.
- The effective thermal conductivity depends on the position and shape of the fibre. As the volume percentage of fibre increases, the effective conductivity increases gradually in radial direction and increases linearly (most likely) in longitudinal direction.
- The iterative homogenisation is most useful for realistic approach since the geometry of fibre in micro scale differs with the geometry of tow in the mesoscale. This method increases the accuracy in terms of volume percentage of fibre.
- The micro and macro voids effects micro and meso saturation. The effective conductivity decreases when the saturation decreases or the volume occupied by the air void increases

### REFERENCES

- [1] R. J. Bascom WDD, ",Microvoids in glass resins composites:their origin and effect on composite strength," Ind Eng Chem Prod Res Dev, pp. 7(3):172-8., 1968.
- [2] J. R. B. L. L. T. Varna J, " Effect of voids on failure machanisms laminates in RTM laminates," Compos Sci Technol , pp. 53:241-9., 1995.
- [3] L. A. S. A. B. J. I. L. W. Park CH, " Modeling and simulation of voids and saturation liquid composite moulding process," Compos Part A: Appl Sci Manuf , pp. 42(6):658-68., 2011.
- [4] G. B. L. C. Lundstrom TS, " Void formation in RTM.," J. Reinf. Plast. Compos., pp. 12(12):1339-49. , 1993.
- [5] R. E. Lecrec JS, "Porosity reduction using optimized flow velocity in resin transfer moulding," Compos Part A: Appl Sci Manuf , pp. 39(12):1859-69., 2008.
- [6] S. G. V. S. N. B. J. B. D. D. Maxime Villiere, "Dynamic saturation curve measurement in liquid composite moulding by heat transfer analysis.," Compos Part A, pp. 69:255-265, 2015.
- [7] N. P. a. LEE, " Effect of Fiber Mat Architecture on void formation and removal in LCM.," Polymer compos, pp. 16(5): 386-399., 1995.
- [8] A. S. T. S. W. a. S. A. RS Parnas, " The interactions between Microscopic and Macroscopic flow in RTM preforms.," Compos Struct, pp. 27:93-107., 1994.

- 
- [9] D. L. V. S. N. B. D. D. M. Villiere, "Experimental Determination and modelling thermal conductivity tensor of carbon/epoxy composite.," *Compos Part A*, pp. 46:60-68, 2012.
- [10] M. E. C. a. J. B. C. E. I. Rodriguez, "Reiterated homogenisation applied to heat conduction in heterogenous media with multiple spatial scales and perfect thermal contact between phases," *J Braz Soc Mech Sci Eng*, no. 10.1..7/s40430-016-0497-7.
- [11] J. L. Auriault, "Heterogenous medium is an equivalent macroscopic description is possible," *Int. J. Engg* , vol. 29, pp. 7:785-795 , 1991.
- [12] J. L. A. a. H. I. ENE, "Macroscopic modelling of heat transfer in composites with interfacial thermal barrier," *Int. J. Engg* , vol. 37, no. 18, pp. 2885-2892., 1994.
- [13] C.-Y. W. a. C. Beckermann, "A two-Phase mixture model of liquid – gas flow and heat transfer in capillary porous media-I formulation," *Int. J. HMT*, vol. 36, no. 11, pp. 2747-2758, 1993.
- [14] L. D. S. L. C. a. J. A. J P Vassal, "Upscaling the diffusion equations in particulate media made of highly conductive particles," *American Physical Theory*, no. 1539-3755/2008/77(1)/011302(10)., 2008.
- [15] M. Kaminski, "Homogenisation of Transient Heat Transfer Problems for Some Composite Materials," *Int. J. Engg. Sci*, no. 41, pp. 1-29, 2003.
- [16] M. Kaviany., *Principles of Heat Transfer in Porous media*, Michigan: springer, 1999.

# Study of the Nickel Complex Formation with Citric Acid in A Mixture Alkyl Polyglycoside10 (APG10) Surfactant/Water System

Do Xuan Truong<sup>1</sup>, Nguyen Van Hoang<sup>2</sup>, To Van Thiep<sup>3</sup>

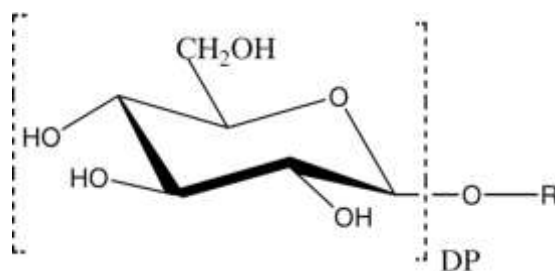
New Technology Institute and Environmental Protection, Academy of Military Science and Technology

**Abstract**— The stability constants of complexes formed by metal cations Ni(II) and citric acid in water and in APG10 surfactant/water medium are determined by the pH titration method combined with using Hyss 2009 simulation software. Under experimental conditions, the Ni(II) complexes with citric acid ligand were determined consisting of  $[NiCit]^-$ ,  $[NiHCit]$ ,  $[NiCit_2]^{4-}$  and  $[NiHCit_2]^{3-}$ . The  $\log\beta$  values of the stability constants of the complex species are linearly dependent and decreases with increasing concentration of APG10. The influence of APG10 surfactant on the decrease of stability constants maybe explained by the interaction of the surfactant micelles with the complex species. In 0.5% APG10/water solution, the decrease in stability constant value of Ni(II) - Citric complexes compared to these values in the aqueous environment are from 4.367 to 14.126 times.

**Keywords**— Stability constant, Complex, Citric acid, APG10 non-ionic surfactant.

## I. INTRODUCTION

The Complexes of metal ions with chelated agents exhibits great concern in many approaches of researches and applications, such as paper production, textiles, medicine, biology and water treatment [1-3]. The complexes of heavy metal ions as such Ni, Co, Sr, U ... with chelating organic ligands in aqueous media were studied [4-7]. The formation of metal ions – chelating organic ligands in mixed surfactant compounds/water is received a great interest due to their advantage of micelles present in media to the possibility varying the complex stability constants [8-10]. In this paper, the nickel Ni(II) complex formation with citric acid in a mixed alkyl polyglycoside (APG10) was studied in detail. Alkyl polyglycoside is a biodegradable ingredient that is growing in popularity due to its favorable environmental profile, is non-ionic surfactant widely used in a variety of cosmetic, household, and industrial applications [11-12]. The raw materials to produce alkyl polyglycoside are typically starch and fat. The final products of this process are typically complex mixtures of compounds with different sugars comprising the hydrophilic end and alkyl groups of hydrophobic. The molecular structure of an alkyl polyglycoside may be presented as following:



Here DP is degree of polymerization (DP)

Ni(II) – Citric acid complex is formed in aqueous media, but the complex stability constant might be influenced by adding APG10. This influence will be studied in detail in this paper. The formation of Ni(II) -Citric acid in the mixed alkyl polyglycoside surfactant/water system can let's applying in practice to clearing the nickel contaminated media like liquid or solid surface. From here, an application of metal – Citric acid complexes to removal of metal ions in any media with the presence of alkyl polyglycosides.

## II. EXPERIMENTAL

### 2.1 Chemicals

Chemicals used in this study involve as follows:

Ni(NO<sub>3</sub>)<sub>2</sub>.6H<sub>2</sub>O, Merck; APG10 non-ionic surfactant (Merck), citric acid, 99%, Indian; 0.1M HNO<sub>3</sub> standard tubes, NaNO<sub>3</sub> (p.A).

## 2.2 Equipment

The equipment and instruments are mainly used: Mettler Toledo S220K pH meter (Switzerland), Cole Palmer heating stirrer, Hyss 2009 simulation computer software.

## 2.3 Methods

The study of the complex formation of citric with metal cations in water and APG10 surfactants was conducted by titration method, combined with Hyss 2009 software [5,6].

TABLE 1

THE RATIO OF COMPONENTS OF THE EXPERIMENTAL SOLUTION TO DETERMINE THE STABILITY CONSTANTS OF THE COMPLEXES WHICH ARE CREATED BY Ni<sup>2+</sup>, WITH CITRIC ACID IN WATER AND APG10 SURFACTANT

Numerical order	V <sub>HNO<sub>3</sub></sub> (mL)	V <sub>H<sub>2</sub>O</sub> (mL)	V <sub>NaNO<sub>3</sub></sub> (mL)	V <sub>citric</sub> (mL)	V <sub>APG10</sub> (mL)	V(Ni(II)) (mL)
1	1.6	66.4	8	4	0	0
2	1.6	53.3	8	4	13.1	0
3	1.6	40.2	8	4	26.2	0
4	1.6	27.0	8	4	39.4	0
5	1.6	13.9	8	4	52.5	0
6	1.6	0.8	8	4	65.6	0
7	1.6	65.6	8	4	0	0.8
8	1.6	52.5	8	4	13.1	0.8
9	1.6	39.4	8	4	26.2	0.8
10	1.6	26.2	8	4	39.4	0.8
11	1.6	13.1	8	4	52.5	0.8
12	1.6	0	8	4	65.6	0.8

Pipette a solution of 0.1M HNO<sub>3</sub>, 1M NaNO<sub>3</sub>, 0.1M citric, 0.1M Ni(II) ions, 0.61% APG10 and water according to Table 1 ratio into a 250 mL glass beaker (total solution used in each experiment was 80 mL).

**Experiment N0.1:** Used to determine the stability constant of citric acid in aqueous solution (without surfactant).

**Experiment N0. 2-6:** Used to determine the stability constant of citric acid in the environment of APG10 surfactant with concentration of APG10 of 0.1%; 0.2%; 0.3%; 0.4%; 0.5%.

**Experiment N0. 7:** To study the complexing of citric acid with metal cations Ni(II), in aqueous environment (without surfactant).

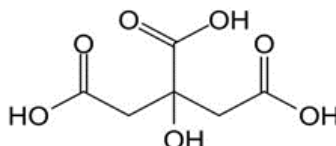
**Experiment N0. 8-12:** To study the complexing of citric acid with metal cations Ni<sup>2+</sup>, Co<sup>2+</sup>, Sr<sup>2+</sup>, Zr<sup>4+</sup> in the environment of APG10 surfactant with concentration of APG10 of 0.1%, 0.2%, 0.3%, 0.4%, 0.5%.

Use a 1000 μL micropipette to drop slowly about 0.2 mL of the 0.1M NaOH solution into a 250 mL glass beaker containing 80 mL of solution in the above experiments. Stir the solution with a magnetic stirrer with a stirring speed of 125 rpm at 30 °C. Wait for the solution to stabilize and measure the pH; record pH values and develop titration curves, in conjunction with Hyss 2009 software [13] to determine the stability constants and the distribution of complex constituents.

## III. RESULTS AND DISCUSSION

### 3.1 The influence of APG10 surfactant on the stability constant of citric acid

Citric is a weak organic acid with molecular formula C<sub>6</sub>H<sub>8</sub>O<sub>7</sub>, structural formula [2]



In solution, citric acid dissociates in 3 steps (denoted by citric acid as  $H_3Cit$ ) to form  $H_2Cit^-$ ,  $HCit^{2-}$  and  $Cit^{3-}$  ions. The stability constants of  $H_3Cit$ ,  $H_2Cit^-$ ,  $HCit^{2-}$  species are denoted  $\beta_{H_3Cit}$ ,  $\beta_{H_2Cit^-}$ ,  $\beta_{HCit^{2-}}$  respectively. The alkalimetric titration curve for citric acid in aqueous medium is given in Figure 1. This titration curve exhibits the acid-base equilibrium is active in the pH range from 2.5 to 11. In experimental solution, citric acid exists in 4 forms:  $H_3Cit$ ,  $H_2Cit^-$ ,  $HCit^{2-}$  and  $Cit^{3-}$ . The ratio of the above species depends on the pH of the environment. When pH increases, the content of  $H_3Cit$  decreases,  $Cit^{3-}$  increases; the content of  $H_2Cit^-$  reaches its maximum at pH = 4 while  $HCit^{2-}$  maximizes at pH = 5.5. When pH > 7, there is only species of  $Cit^{3-}$  in solution (Figure 1b).

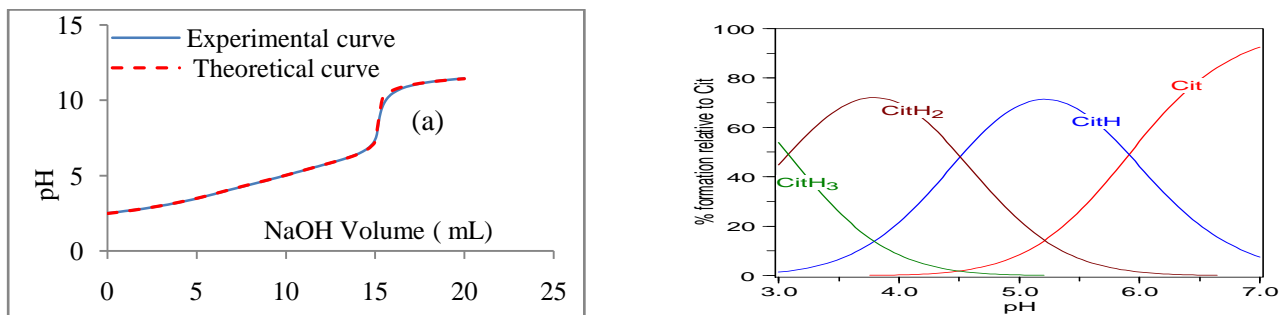


FIGURE 1. Alkalimetric titration curve (1a) and the distribution concentration of citric acid constituents in water (1b).

From the software program, we have determined the stability constant value of citric acid under experimental conditions as shown in Table 2.

TABLE 2  
STABILITY CONSTANTS OF CITRIC ACID IN WATER

Values of	log $\beta$
$HCit^{2-}$	$5,91 \pm 0,05$
$H_2Cit^-$	$10,42 \pm 0,07$
$H_3Cit$	$13,50 \pm 0,08$

By the same method, the stability constants ( $\beta$ ) of these species in mixed AVG 10/water system were determined. The dependence of log  $\beta$  on the APG10 concentration varying from 0 to 0.5% (in water) is represented in Figure 2. Thus, the presence of APG 10 has affected the dissociation of citric acid in water solution. The formation of micelles APG10 might reduce the interaction of citric acid species leading to reduce the stability constants in water. This phenomenon is almost the same as the case that was published in the literature [6].

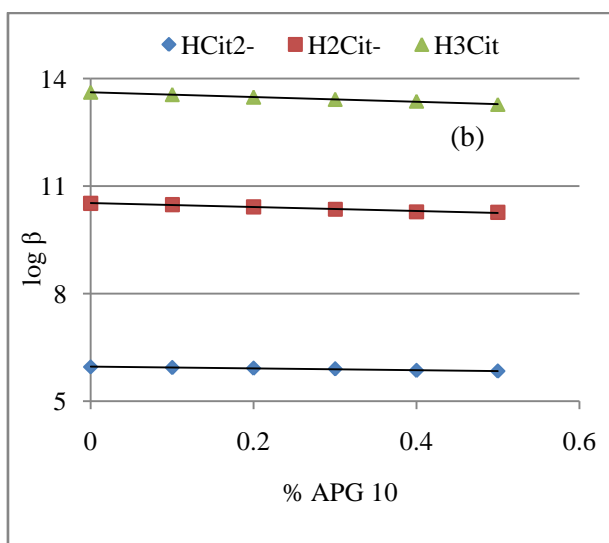


FIGURE 2. The dependence of log  $\beta$  on varying APG 10 concentration

### 3.2 Complexization of Ni(II) ions with citric acid in water

Based on Hyss software, under experimental conditions, the species of complexes of Ni(II) with Citric acid were determined, consisting of  $[\text{NiCit}]^-$ ,  $[\text{NiHCit}]$ ,  $[\text{NiCit}_2]^{4-}$  and  $[\text{NiHCit}_2]^{3-}$ . The species of complexes depend on the pH of the solution.

From Figure 3, there are  $[\text{NiCitH}]$  and  $[\text{NiCit}_2\text{H}]^{3-}$  at pH of 3-4,  $[\text{NiCit}]^-$  and  $[\text{NiCit}_2]^{4-}$  complexes at pH of 6. At pH > 7 there is only form of  $[\text{NiCit}_2]^{4-}$ .

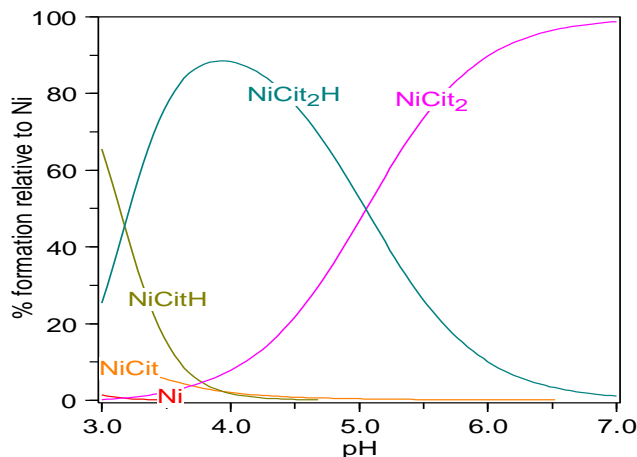


FIGURE 3. The species of Ni(II)-Cit complex compounds in aqueous medium

### 3.3 Complexization of Ni(II) ions with citric acid in APG10/Water medium

From the alkalimetric titration curve (Figure 4) the stability constants of Ni(II)-Cit species in APG10 surfactant /water solution were determined and presented in Table 3.

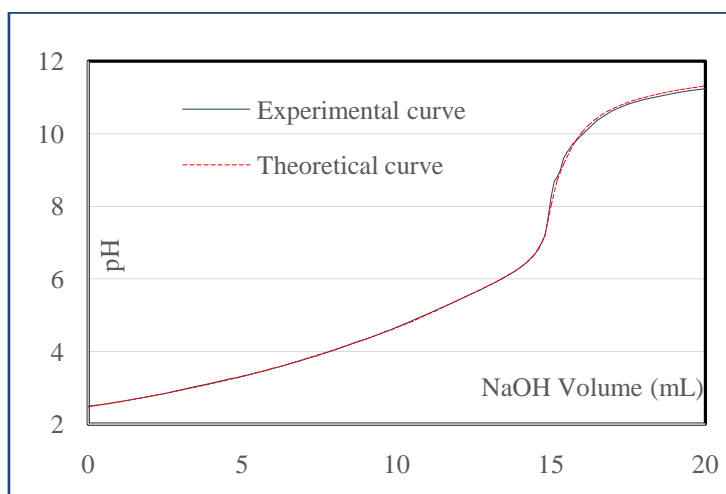
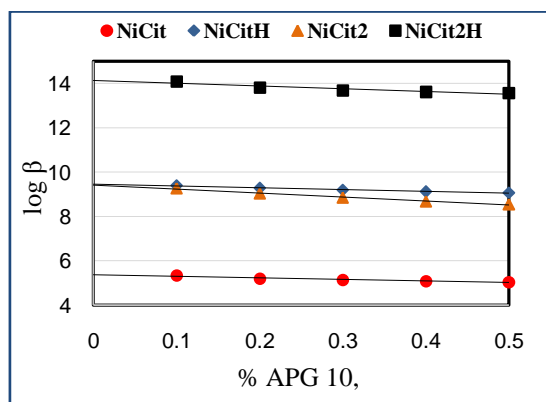


FIGURE 4. Alkalimetric titration curve of Ni(II)-Cit in APG10 surfactant /water system.

TABLE 3  
DEPENDENCE OF THE STABILITY CONSTANTS OF COMPLEX SPECIES FORMED BY Ni(II) AND CITRIC ACID IN VARYING APG10 CONCENTRATIONS

APG 10(%)	$\beta$			
	$\text{NiCit}^-$	$\text{NiCitH}$	$\text{NiCit}_2^{4-}$	$\text{NiCit}_2\text{H}^{3-}$
0	$4.79 \cdot 10^5$	$6.61 \cdot 10^9$	$5.01 \cdot 10^9$	$3.55 \cdot 10^{14}$
0.1	$2.19 \cdot 10^5$	$2.51 \cdot 10^9$	$1.86 \cdot 10^9$	$1.23 \cdot 10^{14}$
0.2	$1.58 \cdot 10^5$	$1.90 \cdot 10^9$	$1.10 \cdot 10^9$	$6.61 \cdot 10^{13}$
0.3	$1.38 \cdot 10^5$	$1.58 \cdot 10^9$	$7.08 \cdot 10^8$	$4.90 \cdot 10^{13}$
0.4	$1.20 \cdot 10^5$	$1.32 \cdot 10^9$	$4.79 \cdot 10^8$	$4.07 \cdot 10^{13}$
0.5	$1.10 \cdot 10^5$	$1.17 \cdot 10^9$	$3.55 \cdot 10^8$	$3.71 \cdot 10^{13}$

The results of Table 3 shows, with APG10 concentration increasing, the stability constant of complex species decrease. The stability constant values of  $[\text{NiCit}]^-$ ,  $[\text{NiCitH}]$ ,  $[\text{NiCit}_2]^{4-}$ ,  $[\text{NiCit}_2\text{H}]^{3-}$  at 0.5% APG, respectively decrease to 4.367; 5.623; 14.126; 9.550 times compared to the values in the absence of surfactants, respectively. The dependence of  $\log \beta$  on APG10 concentration varying is presented in Figure 5.



**FIGURE 5. The dependence of  $\log \beta$  of complexes formed between metal ions Ni(II) and citric acid in APG10/water solution.**

The Figure 5 shows,  $\log \beta$  is linearly decreasing on APG10 concentration increasing. This can be explained by the formation of APG 10 micelles leading to the distribution of complex species into different micelle phases, hindering the combination of complex components so the stability constant decreases. An increase in the concentration of APG10 leads to a change in shape and an increase in micelle size, which leads to a decrease in the stability constant, similarly published in [6, 14, 15].

#### IV. CONCLUSION

In the environment of APG10 surfactants/water system, the metal ions Ni(II) form complexes with citric acid in the same complex form as in the aqueous medium. However, the constituent content of citric acid, complexes and the stability constant values have changed. For citric acid, when the concentration of APG10 increased to 0.5% of the values  $\beta(\text{H}_3\text{Cit})$ ,  $\beta(\text{H}_2\text{Cit})$ ,  $\beta(\text{HCit}^{2-})$  decreased by 2.188; 1.778; 1.318 times compared with the stability constant value in water environment. For  $\text{Ni}^{2+}$  complexes, this value decreases gradually for  $[\text{NiCit}]^-$ ,  $[\text{NiCitH}]$ ,  $[\text{NiCit}_2]^{4-}$ ,  $[\text{NiCit}_2\text{H}]^{3-}$  complexes, being 4.367; 5.623 ; 14.126 ; 9.550 times respectively at APG10 0.5%.

#### REFERENCES

- [1] Nethala Vijaya Kumar, Bathula Sreekanth and Gollapalli Nageswara Rao, Speciation of L-Aspartic acid complexes of Co(II), Ni(II), Cu(II) and Zn(II) in acetonitrile and ethylene glycol – water. 2012, Bull. Chem. Soc. Ethiop. 26(2), 239-247.
- [2] Bathula Srikanth, Pedada Srinivasa Rao, Vasa Samba Siva Rao, Charla Kamala Sastry and Gollapalli Nageswara Rao. Effect of micelles on the chemical speciation of binary complexes of Co(II), Ni(II), Cu(II) and Zn(II) with succinic acid, 2009, J. Serb. Chem. Soc. 74 (7) 745–754 (2009), JSCS–3872.
- [3] M. Padma Latha, V. Maheswara Rao, T. Siva Rao and G. Nageswara Rao Chemical speciation of Pb(II), Cd(I), Hg(II), Co(II), Ni(II), Cu(II) and Zn(II) binary complexes of L-methionine in 1,2 propanediol-water mixture. 2007, Bull. Chem. Soc. Ethiop., 21(3), 363-372.
- [4] D. Wyrzykowski • L . Chmurzynski Thermodynamics of citrate complexation with  $\text{Mn}^{2+}$ ,  $\text{Co}^{2+}$ ,  $\text{Ni}^{2+}$  and  $\text{Zn}^{2+}$  ions, J. Therm Anal Calorim (2010) 102:61–64, DOI 10.1007/s10973-009-0523-4.
- [5] Malla Ramanaiiah S. Goutham Sri and B.B.V. Sailaja Stability of binary complexes of Pb(II), Cd(II) AND Hg(II) with maleic acid in TX 100- water mixtures. Bull. Chem. Soc. Ethiop. 2014, 28(3), 383-391. ISSN 1011-3924.
- [6] Srinivasa Rao Pedada, Srikanth Bathula, Samba Siva Rao Vasa, Kamala Sastry Charla and Nageswara Rao Gollapalli\* Micellar effect on metal –ligand complexes of Co(II), Ni(II), Cu(II) AND Zn(II) with acid citric. Bull. Chem. Soc. Ethiop. 2009, 23(3), 347-358.
- [7] W von Rybinski; K Hill (1998). "Alkyl Polyglycosides—Properties and Applications of a new Class of Surfactants". Angewandte Chemie International Edition. 37 (10): 1328–1345,
- [8] Gang Li, Lifeng Chen, Yang Ruan, Qiao Guo, Xingao Liao & Bowen Zhang Alkyl polyglycoside: a green and efficient surfactant for enhancing heavy oil recovery at high-temperature and high-salinity condition, *Journal of Petroleum Exploration and Production Technology* volume 9, pages2671–2680(2019).
- [9] Dorota Kolodyńska, *Chelating Agents of a New Generation as an Alternative to Conventional Chelators for Heavy Metal Ions Removal from Different Waste Waters*, Maria Curie-Skłodowska University, Poland (2011).

- [10] John Drake, *Evaluation of nine chemical-based technologies for removal of radiological contamination from concrete surfaces*, U.S. Environmental Protection Agency (EPA), pp. 3 (2011).
- [11] Rakesh M. Tada\*, Pankaj B. Nariya, Naimish K. Chavda and Manish K. Shah, *Evaluation of stability constants of 1-(3-bromo-4-hydroxy-5-methoxy benzylidene) thiosemicarbazide(TRM-1) with copper (II), cobalt (II) and nickel (II) complexes by pH metric method*, Der Pharma Chemica, **5(4)**, 244-251 (2013).
- [12] Surya Sunitha P1, Nageswara Rao Ch2\*, Sujatha P3, and Sailaja BBV, *Formation and Confirmation of Binary Complexes of Co (II), Ni (II) and Cu (II) with L-Cysteine in SLS-water media*, Research Journal of Pharmaceutical, Biological and Chemical Science (2017).
- [13] Lucia Alderighi a , Peter Gans b,\* , Andrea Ienco a , Daniel Peters, Antonio Sabatini a , Alberto Vacca. Hyperquad simulation and speciation (HySS): a utility program for the investigation of equilibria involving soluble and partially soluble species. *Coordination Chemistry Reviews* 184 (1999) 311–318.
- [14] Greisser, R. and Sigel, H. 1970. Ternary complexes in solutionVIII: complex formation between the copper(II) -2, 20 -bipyridyl 1 : 1 complex and ligands containing oxygen and(or) nitrogen donor atoms. *Inorg. Chem.*, 9, 1238 – 1243. Greisser, R. and Sigel, H. 1971. Ternary complexes in solution.
- [15] Greisser, R. and Sigel, H. 1974. Ternary complexes in solutionXVI: Influence of the size of the chelate rings on the stability of mixed ligand copper(II) complexes containing aliphatic ligands. *Inorg. Chem.*, 13, 462 – 465.





**AD Publications**

**Sector-3, MP Nagar, Bikaner,  
Rajasthan, India**

**[www.adpublications.org](http://www.adpublications.org), [info@adpublications.org](mailto:info@adpublications.org)**